

New pyrimidine and pyridine derivatives as multitarget cholinesterases inhibitors: design, synthesis, *in vitro* and *in cellulo* evaluation

Martina Bortolami ^a, Fabiana Pandolfi ^a, Valeria Tudino ^b, Antonella Messori ^b, Valentina Noemi Madia ^b, Daniela De Vita ^c, Roberto Di Santo ^{a, d}, Roberta Costi ^{a, d}, Isabella Romeo ^{e, f}, Stefano Alcaro ^{e, f, *}, Marisa Colone ^g, Annarita Stringaro ^g, Alba Espargaró ^h, Raimon Sabatè ^h, Luigi Scipione ^{a, *}

^a Department of Scienze di Base e Applicate per l'Ingegneria, Sapienza University of Rome,
via Castro Laurenziano 7, I-00161, Rome, Italy

^b Department of Chimica e Tecnologia del Farmaco, Sapienza University of Rome, Piazzale
Aldo Moro 5, 00185, Rome, Italy

^c Department of Environmental Biology, Sapienza University of Rome, Piazzale Aldo Moro
5, 00185, Rome, Italy

^d Istituto Pasteur, Fondazione Cenci Bolognetti, Department of Chemistry and Technology of
Drug, Sapienza University of Rome, Piazzale Aldo Moro 5, 00185, Rome, Italy

^e Net4Science s.r.l., Campus universitario "S. Venuta", Viale Europa, 88100, Catanzaro, Italy

^f Dipartimento di Scienze della Salute, Università "Magna Græcia" di Catanzaro, Viale
Europa, 88100, Catanzaro, Italy

^g National Center for Drug Research and Evaluation, Istituto Superiore di Sanità, Viale
Regina Elena, 00161, Rome, Italy

^h Department of Pharmacy and Pharmaceutical Technology and Physical-Chemistry, Faculty
of Pharmacy and Food Sciences, University of Barcelona, Avda. Joan XXIII, 27-31
Barcelona, Catalonia, Spain

ABSTRACT

A new series of pyrimidine and pyridine diamines was designed as dual binding site inhibitors of ChEs, characterized by two small aromatic moieties separated by a diaminoalkyl flexible linker. Many compounds are mixed or uncompetitive AChE and/or BChE nanomolar inhibitors, being compound **9** the most active on *Ee*AChE ($K_i = 0.312 \mu\text{M}$) and compound **22** on *eq*BChE ($K_i = 0.099 \mu\text{M}$). Molecular docking and molecular dynamic studies confirmed the interactions mode of our compounds with the enzymatic active site. UV-Vis spectroscopic studies showed that these compounds can form complexes with Cu^{2+} and Fe^{3+} and that compounds **18**, **20** and **30** have antioxidant properties. Interestingly, some compounds were also able to reduce $\text{A}\beta_{42}$ and Tau aggregation, with compound **28** being the most potent (22.3% and 17.0% inhibition on $\text{A}\beta_{42}$ and Tau, respectively). Moreover, the most active compounds showed low cytotoxicity on human brain cell line and they were predicted as BBB-permeable.

KEYWORDS. Acetylcholinesterase inhibitors, Butyrylcholinesterase inhibitors, multitarget compounds, amyloid aggregation, Tau aggregation, metal chelation, antioxidant

Introduction

Alzheimer's disease (AD) is one of the most serious and prevalent neurodegenerative diseases; it accounts for the 50-75% of dementia in humans, currently affecting 44 million people worldwide,¹ and causes huge social economic losses.² In 2015, the World Alzheimer Report estimated over 9.9 million new cases of dementia each year (approximately one new case every 3 seconds), that allows to predict a population of 70 million by 2030, which could rise to 130 million by 2050.³ AD begins with short-term memory loss followed by a progressive decline in memory and cognitive ability, associated with severe behavioural abnormalities, such as irritability, anxiety and depression, and the outcome is always fatal.

Although the precise pathogenetic mechanisms of AD remain to be elucidated, several factors appear to play key roles in the onset and progression of the AD and they comprise: the cholinergic deficit, with reduced levels of acetylcholine (ACh) and many cholinergic markers; the β -amyloid peptide ($A\beta$) deposition; the hyperphosphorylation and the deposition of Tau protein; the dysregulation of energy metabolism and the increase in oxidative stress; the dyshomeostasis of biometals; and the neuroinflammation.⁴ The cholinergic hypothesis, the first approach developed to describe the pathophysiology of AD, is based on three main evidences observed in AD patients: i) a severe neurodegeneration of the nucleus basalis of Meynert, main source of cortical cholinergic innervation; ii) a severe depletion of the presynaptic cholinergic markers, such as choline acetyl transferase (ChAT); iii) the cholinergic antagonist drugs induce memory impairment and cognitive deficits that are alleviated by cholinergic agonists.⁵⁻⁸

These evidences have led to the therapeutic use in AD of cholinesterase inhibitors (ChEIs), able to restore cholinergic tone by blocking the cholinesterases (ChEs) activity and consequently increasing the availability of ACh at the synaptic cleft.

To date, the ChEIs remain the primary therapy for AD, with donepezil, galantamine and rivastigmine, currently approved by the Food and Drug Administration (FDA), along with the

NMDA receptor antagonist memantine.⁹ Unfortunately, these drugs have shown limited clinical results, with short-lasting positive effects and the lack of ability to stop the progression of the disease. The absence of decisive and long-term effects stimulates researchers to develop new therapeutic strategies with the objective of restoring cerebral cholinergic activity, as the degeneration of the cortical cholinergic projection represents a key irreversible event in the progression of AD.

At the neuronal level, there are two types of ChEs: acetylcholinesterase (AChE) and butyrylcholinesterase (BChE). AChE activity is dominant in the healthy brain (80%), while BChE exerts a supportive role. However, with the progression of the disease, brain levels of AChE decline approximately to 60% while those of BChE increase to 120% of normal levels, thus suggesting for the latter a major role in the severe forms of the disease and the possibility of considering it an adequate therapeutic target of AD.^{10, 11}

AChE and BChE have 65% amino acid sequence identity; they possess a catalytic active site (CAS), located at the bottom of a 20 Å gorge, constituted by a catalytic triad: Ser203, His447 and Glu202 in human AChE (*hAChE*) and Ser198, His438 and Glu197 in human BChE (*hBChE*). An anionic sub-site is also present that is constituted by Trp86 in *hAChE* and Trp82 in *hBChE*, which bind the quaternary ammonium of ACh moiety, by means of cation- π interaction.^{12, 13} These enzymes exhibit an allosteric modulation site, the peripheral anionic site (PAS), located at the entrance of the active site gorge, that in *hAChE* consists of five residues, Tyr72, Asp74, Tyr124, Trp286 and Tyr341, while in *hBChE* is constituted by Tyr332 and Asp70.^{14, 15} Beside its role in the modulation of the catalytic activity, PAS has been reported to be involved in the pro-aggregating action of AChE toward A β peptide, another important actor in the onset and progression of AD.^{16, 17}

The growing scientific evidences highlighting the close correlation between the severe cholinergic depletion and the other pathophysiological events observed in AD, particularly

with the abnormal A β and Tau cascade, give a new interest to the development of new ChEIs for the treatment of AD, and in particular towards multitarget compounds, able to act simultaneously at more levels on the different mechanisms involved in the pathogenesis of AD.¹⁸ Many reviews available in the scientific literature summarize the main research lines followed in the development of multitarget compounds for the therapy of AD, both in the academic and industrial fields. The majority of articles and patents report studies on dual binding site ChEIs that are able to interact both with CAS and PAS of these enzymes and are endowed with the activity on one or more additional targets, such as a second neurotransmitter system (*i.e.*, serotonergic or monoaminergic), or A β and Tau production and deposition, the reduction of oxidative stress or biometals dyshomeostasis.¹⁹⁻²¹

In our previous studies, we synthesized and *in vitro* evaluated new series of dual binding site ChEIs, characterized by two small aromatic moieties separated by various functionalized linker, some of which resulted nanomolar mixed or uncompetitive inhibitors of both AChE and BChE, able to bind CAS and PAS, able to reduce A β aggregation or endowed with metal chelating properties.^{22, 23}

Based on these considerations and as a development of previous works, we decide to study a new series of pyrimidine and pyridine diamine derivatives and evaluate them both *in vitro* and *in cellulo*, as potential ChEIs endowed with chelating and antioxidant activities as well as direct anti-amyloid aggregation properties, with the aim to develop new multifunctional compounds for AD. These molecules were designed as dual binding site inhibitors, based on the structure of ChEs enzymatic pocket, inserting two small aromatic groups separated by an aliphatic linker (Figure 1). The aromatic moieties are potentially able to interact with the aromatic amino acids located adjacent to the CAS and in the PAS of the enzymes by means of π - π interactions, while the aliphatic linker covers the distance between CAS and PAS and gives flexibility to the compounds. Due to the difficulty to predict the conformational behavior of

linear alkyl chains, different length linkers were used, in particular with five or six methylene units. Within the chain a protonable amine group, both acceptor and donor of hydrogen bond and able to establish cationic- π interactions with the aromatic residues of the enzymes, was inserted in order to promote interactions with the amino acids of the enzymes gorge. A 2-amino-pyrimidinic or 2-amino-pyridinic moiety was introduced as one of the two aromatic groups, since the presence of the two adjacent nitrogen atoms could confer chelating activity to the compounds. On the other side of the aliphatic chain different aromatic groups have been chosen, with the purpose of acquiring further information about the structural requirements for targeting ChEs. Among these groups also phenolic or catecholic rings have been selected to enhance chelating properties and to confer direct antioxidant activity.

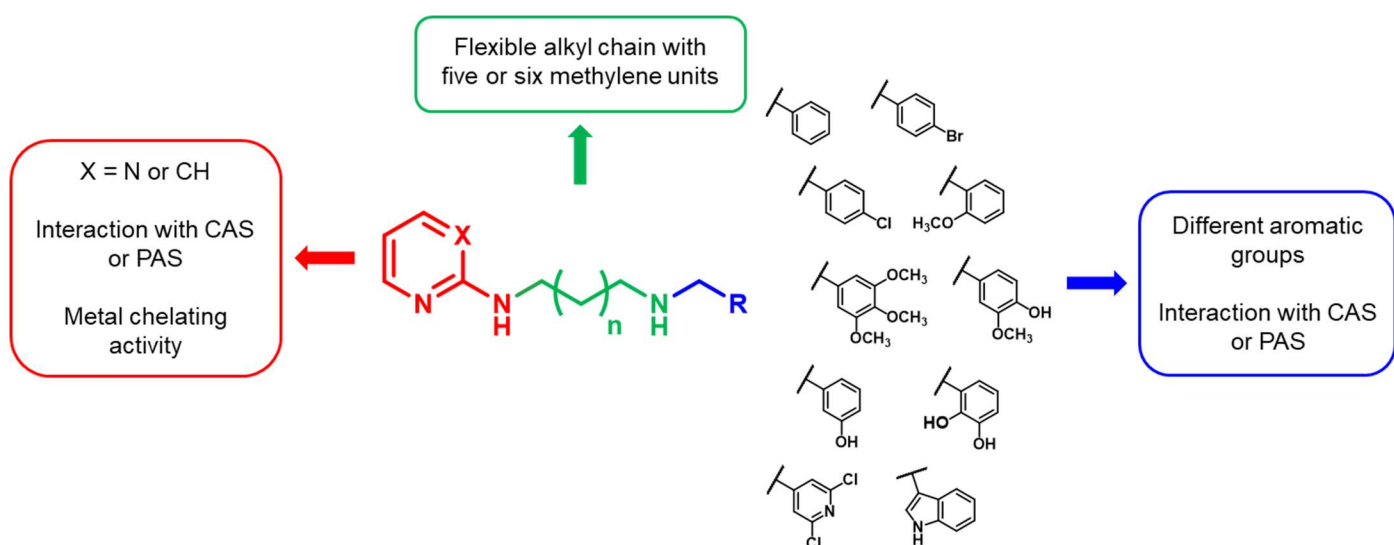


Figure 1. Rational design of the 2-amino-pyrimidine or 2-amino-pyridine derivatives.

Results and discussion

Chemistry. *General procedure for the synthesis of pyrimidine diamine derivatives 9-22.*

The pyrimidine diamine derivatives **9-22** were synthesized following the procedures described in Scheme 1. Initially the intermediates **3** and **4** were synthesized through two reaction steps (first method, GP-A and procedure 1 or 2 of GP-B in experimental section);

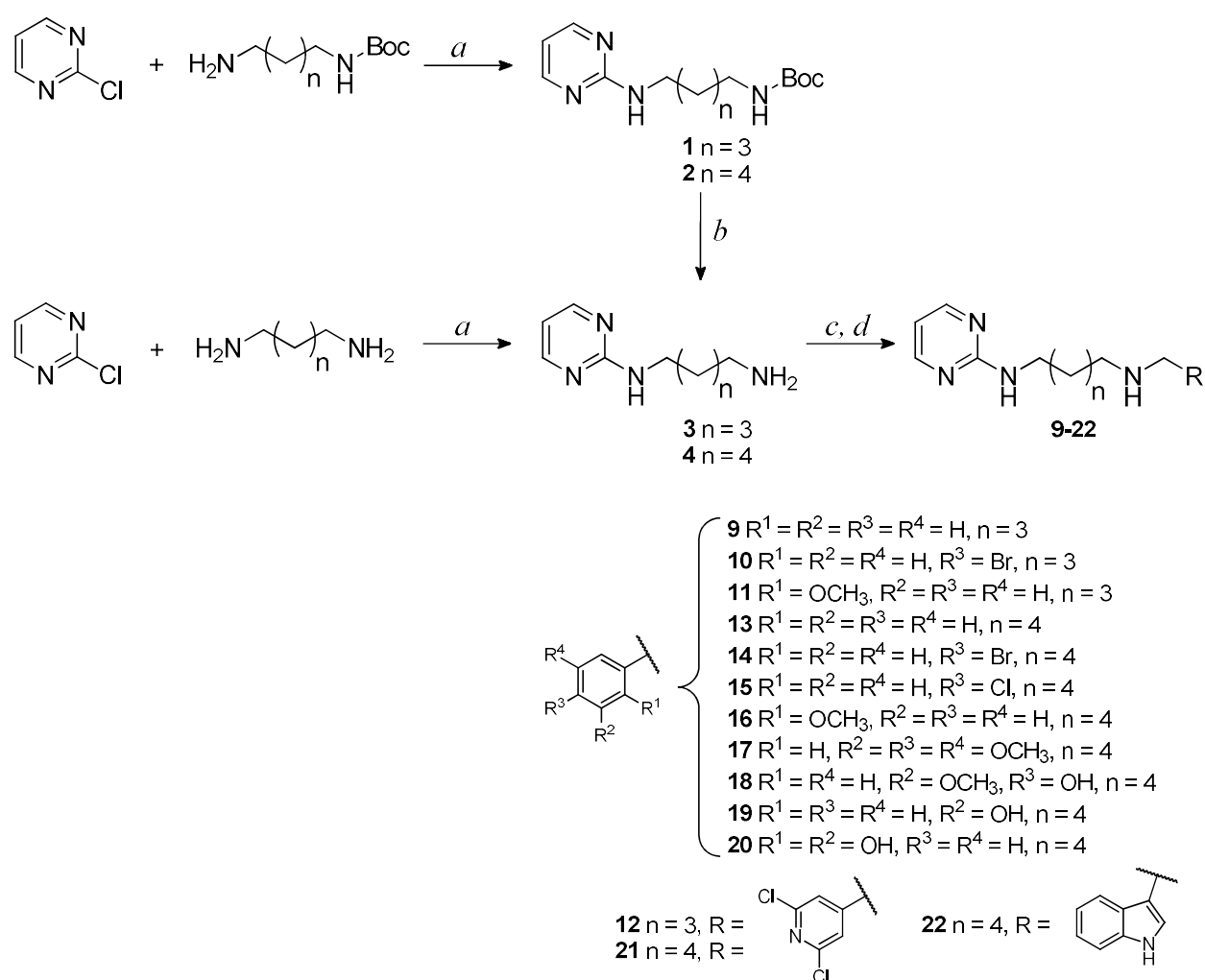
subsequently the intermediate **4** was also obtained directly through a single reaction (second method, procedure 3 of GP-B in experimental section). Following the first synthetic method equimolar amounts of 2-chloropyrimidine, *N*-Boc-1,5-diaminopentane or *N*-Boc-1,6-diaminohexane and triethylamine (TEA) were reacted in methanol at reflux overnight to give the compounds **1** or **2**, which were purified by column chromatography on silica gel. Then the intermediates **1** and **2** were deprotected from Boc by treatment with a high excess of trifluoroacetic acid (TFA) in anhydrous dichloromethane, to obtain the compounds **3** and **4**, which were used either as trifluoroacetic salts or as free amines. According to the second synthetic method, the intermediate **4** was synthesized directly by reaction between 2-chloropyrimidine and an excess of 1,6-diaminohexane in presence of TEA, in methanol at reflux overnight. The excess of diamine allowed to obtain mainly the product of interest, in which only one amino group reacted with 2-chloropyrimidine. The reaction was monitored by ESI-MS and the crude residue was purified by column chromatography on silica gel. The second method proved to be more advantageous than the first, as through a single step it was possible to synthesize the desired pyrimidine intermediate with a higher yield.

Equimolar amounts of the amine intermediates **3** or **4** and the appropriate aldehyde were dissolved in dry dichloromethane in presence of potassium carbonate or molecular sieves as desiccant agents. The choice of the suitable drying agent was based on the starting reagents: when compounds **3** or **4** were used as trifluoroacetic salts, potassium carbonate was utilized both as a desiccant, either as a base to deprotonate the amino groups of the intermediates; when the reaction was carried out using aldehydes containing groups susceptible to acid-base reactions with potassium carbonate (such as indole -NH or phenol -OH), molecular sieves were selected as desiccant agents. These reactions were monitored by IR spectroscopy to confirm the imine formation, with stretching absorption band around 1640 cm^{-1} , and the disappearance of the aldehyde band at about 1700 cm^{-1} . The obtained imine intermediates were reduced by treatment

with sodium borohydride in methanol and after the reaction the excess of sodium borohydride was decomposed by addition of water or 1M HCl. The addition of hydrochloric acid was necessary to avoid oxidation of phenolic derivatives at basic pH.

The residues obtained were purified by column chromatography on silica gel and/or by crystallization. Moreover, the structures of final compounds were confirmed by spectroscopic analysis; as an example in the $^1\text{H-NMR}$ spectra the appearance of the methylene singlet between 3.89-3.63 ppm was observed. The detailed synthetic procedures, the analytical and spectroscopic data of synthesized compounds are reported in the experimental section and agree with the proposed structures.

Scheme 1. Synthetic Route to Pyrimidine Diamine 9-22 Derivatives^a



^a Reagents and conditions: *a*) TEA (1 eq), MeOH, reflux, 20 h; *b*) TFA (20 eq), dry CH₂Cl₂, room temp, 3.5 h; *c*) opportune aldehyde (1 eq), dry CH₂Cl₂, dry K₂CO₃ (for **9-16** and **21**) or activated molecular sieves (for **17-20** and **22**), room temp, 12 h; *d*) NaBH₄ (3 eq), MeOH, room temp, 2 h.

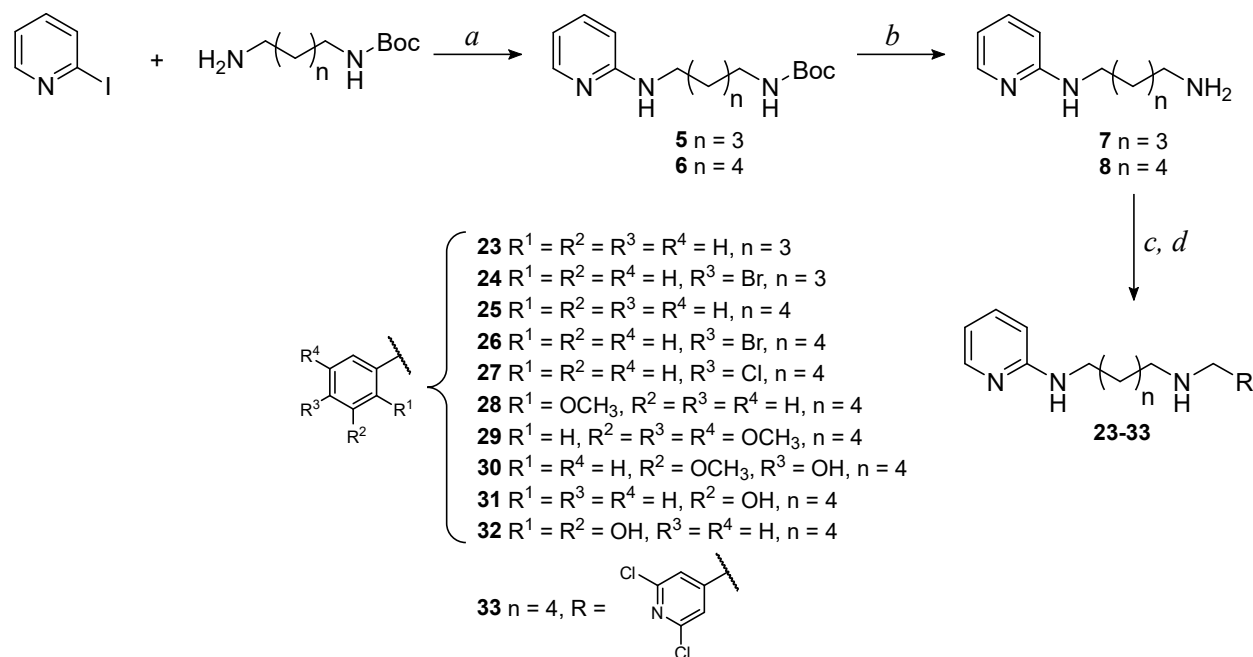
General procedure for the synthesis of pyridine diamine derivatives 23-33.

The pyridine diamine derivatives **23-33** were synthesized following the procedures described in Scheme 2. The intermediates **5** and **6** were obtained by Ullmann coupling catalyzed by CuI and 2-isobutyrylcyclohexanone, as described by Shafir A. and Buchwald S.L.²⁴ A Schlenk flask was charged with *N*-Boc-1,5-diaminopentane or *N*-Boc-1,6-diaminohexane and solid reactants (CuI and Cs₂CO₃) and then it was evacuated and backfilled with N₂. Under a counter flow of N₂, 2-iodopyridine, dimethylformamide (DMF) and finally 2-isobutyrylcyclohexanone were added. The reaction was monitored by ESI-MS and the best yield was obtained stirring the mixture at 40 °C for 21 hours. Purification by column chromatography on silica gel led to the isolation of the products of interest with quantitative yield. Then intermediate **5** and **6** were deprotected from Boc by treatment with a high excess of TFA in anhydrous dichloromethane, to obtain compounds **7** and **8**, which were used either as trifluoroacetic salts or as free amines. Differently from what has been said for the pyrimidine intermediates, in this case it was not possible to synthesize compounds **5** and **6** directly through a single reaction between 2-iodopyridine and an excess of the opportune diamine. In fact, in this way the product in which both amino groups reacted with 2-iodopyridine was mainly obtained.

Then intermediates **7** and **8** were reacted with the appropriate aldehydes and the imines obtained were reduced with sodium borohydride, as previously described for the pyrimidine derivatives. The residues obtained were purified by column chromatography on silica gel or by crystallization. The structures of final compounds were confirmed by spectroscopic analysis; as an example, in the ¹H-NMR spectra the appearance of the methylene singlet between 3.90-3.63 ppm was observed. The detailed synthetic procedures, the analytical and spectroscopic

data of synthesized compounds are reported in the experimental section and agree with the proposed structures.

Scheme 2. Synthetic Route to Pyridine Diamine **23-33** Derivatives^a



^aReagents and conditions: *a*) CuI (0.05 eq), Cs₂CO₃ (2 eq), 2-isobutyrylcyclohexanone (0.2 eq), DMF, N₂, 40°C, 21 h; *b*) TFA (20 eq), dry CH₂Cl₂, room temp, 3.5 h; *c*) opportune aldehyde (1 eq), dry CH₂Cl₂, dry K₂CO₃ (for **23-28** and **33**) or activated molecular sieves (for **29-32**), room temp, 12 h; *d*) NaBH₄ (3 eq), MeOH, room temp, 2 h.

Enzymatic assays.

On the synthesized compounds enzymatic inhibition studies were carried out towards *Electrophorus electricus* AChE (*Ee*AChE) and equine BChE (*eq*BChE) according to the Ellman's spectrophotometric method.²⁵ Initially, for each compound, the percentages of inhibition were determined at the inhibitor concentration equal to 9 μM and, for the most potent compounds, also at 900 nM and 90 nM, in presence of 0.0833 U/mL of enzyme and 100 μM of acetylthiocholine.

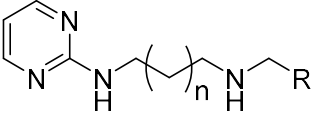
Based on the results illustrated in Table 1, related to pyrimidine diamine derivatives, there are not significant differences between the percentages of inhibition towards *Ee*AChE of the

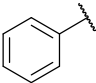
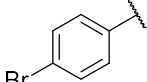
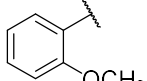
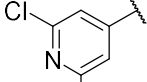
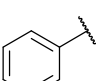
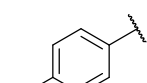
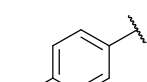
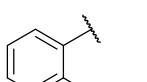
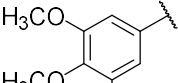
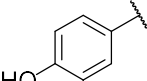
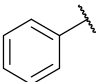
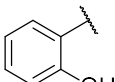
compounds having an aliphatic linker with five methylene units (**9-12**) compared to the corresponding derivatives with six methylene units (**13, 14, 16, 21**). On the other hand, towards *eqBChE* the compounds having a five-methylene chain show a lower inhibitory potency compared to the six methylene derivatives. As a consequence of this observation, for the synthesis of the subsequent compounds we decided to use an aliphatic linker with six methylene units.

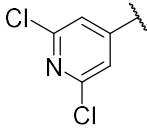
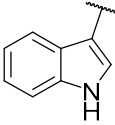
Among pyrimidine diamine derivatives the most potent compounds on *EeAChE*, with approximately 90% of inhibition at 9 μ M, and between 40-60% at 900 nM, are **9** and **13**, both with an unsubstituted phenyl ring on one side of the aliphatic chain, **19**, with a 3-hydroxyphenyl ring, and **20**, having a 2,3-dihydroxyphenyl ring. The insertion of a halogen atom in para position of the phenyl ring (compounds **10, 14** and **15**) as well as the replacement of the phenyl with 3,4,5-trimethoxyphenyl (**17**) or 2,6-dichloropyridine ring (**12** and **21**) cause a drastic reduction of the inhibitory potency on *EeAChE*; the replacement of the phenyl with 2-methoxyphenyl (**11** and **16**), or 3-methoxy-4-hydroxyphenyl (**18**) or indole (**22**) ring reduces the percentages of inhibition towards *EeAChE* from 90% to 60-70% at inhibitor concentration of 9 μ M.

Generally, these pyrimidine diamine derivatives have low inhibitory potency towards *eqBChE* (8-45% at 9 μ M), with the exception of the compound **18**, with 3-methoxy-4-hydroxyphenyl ring, that shows 84% of inhibition at 9 μ M and 44% at 900 nM, and **22**, with indole group, having a 94% of inhibition at 9 μ M and 65% at 900 nM.

Table 1. Inhibition of *EeAChE* and *eqBChE* activities by pyrimidine diamine derivatives **9-22**.

	% inhibition vs <i>EeAChE</i> \pm SD ^a	% inhibition vs <i>eqBChE</i> \pm SD ^a

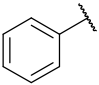
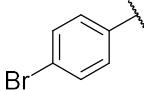
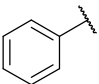
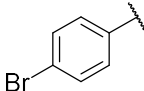
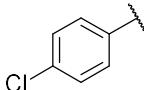
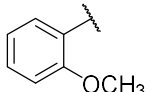
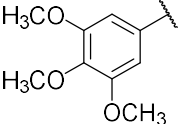
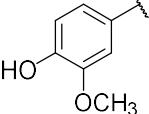
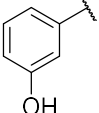
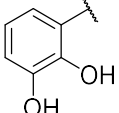
Cmp	R	n	[I] 9 μ M	[I] 900 nM	[I] 90 nM	[I] 9 μ M	[I] 900 nM
9		3	90.2 \pm 0.7	57.1 \pm 0.9	14.1 \pm 1.4	17.4 \pm 2.7	nd ^b
10		3	14.5 \pm 0.7	nd ^b	nd ^b	17.1 \pm 0.9	nd ^b
11		3	62.2 \pm 0.9	14.6 \pm 0.6	nd ^b	22.1 \pm 1.3	nd ^b
12		3	16.5 \pm 2.0	nd ^b	nd ^b	8.5 \pm 1.3	nd ^b
13		4	92.9 \pm 0.4	60.3 \pm 1.5	19.2 \pm 1.4	26.0 \pm 3.5	nd ^b
14		4	23.0 \pm 1.6	nd ^b	nd ^b	38.6 \pm 5.5	6.6 \pm 0.2
15		4	29.9 \pm 1.2	nd ^b	nd ^b	21.5 \pm 1.2	nd ^b
16		4	68.3 \pm 0.7	15.7 \pm 1.1	nd ^b	43.9 \pm 4.8	6.2 \pm 0.4
17		4	16.4 \pm 2.8	nd ^b	nd ^b	29.4 \pm 4.5	nd ^b
18		4	59.5 \pm 3.6	14.7 \pm 0.5	nd ^b	84.4 \pm 0.8	44.2 \pm 6.4
19		4	84.4 \pm 0.3	39.0 \pm 1.9	nd ^b	26.6 \pm 3.9	nd ^b
20		4	90.5 \pm 0.5	53.6 \pm 3.1	12.8 \pm 1.9	17.1 \pm 1.6	nd ^b

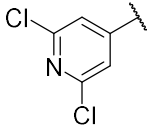
21		4	18.5 ± 1.8	nd ^b	nd ^b	26.8 ± 0.4	nd ^b
22		4	69.2 ± 1.4	16.4 ± 1.9	nd ^b	94.0 ± 0.7	65.1 ± 3.8
	Tacrine		100	97.6 ± 0.1	76.6 ± 0.2	100	99.7 ± 0.3

^a Data are the average of three replicates; ^b nd stands for not determined

Among pyridine diamine derivatives, whose data are reported in Table 2, the compounds having an aliphatic chain with five methylene units (**23** and **24**) show a lower inhibitory potency towards both enzymes compared to the corresponding derivatives with six methylene chain (**25** and **26**). Generally, pyridine diamine derivatives have similar or lower percentages of inhibition on *EeAChE* compared to the corresponding pyrimidine derivatives (Table 1 and 2) with the exception of **29** and **33**, having 3,4,5-trimethoxyphenyl or 2,6-dichloropyridine ring, respectively. On the contrary pyridine derivatives are more potent on *eqBChE* than the corresponding pyrimidine compounds. Among pyridine derivatives the most potent compound on *EeAChE* is **25**, having an unsubstituted phenyl ring on one side of the aliphatic chain, with a 73% of inhibition at 9 μM. Among the compounds with six methylene units the insertion of a halogen atom in para position on the phenyl ring (**26** and **27**) as well as the replacement of the phenyl with 3,4,5-trimethoxyphenyl group (**29**) cause a reduction of the percent inhibition at 9 μM on *EeAChE* from 73% to 24-30%. Furthermore, the replacement of the phenyl with 2-methoxyphenyl (**28**) or 3-methoxy-4-hydroxyphenyl (**30**) or 2,3-dihydroxyphenyl (**32**) ring reduces inhibition at 9 μM to about 60%, while the replacement with 3-hydroxyphenyl (**31**) or 2,6-dichloropyridine (**33**) ring reduces inhibition to about 40%. On *eqBChE* the most potent compound is **30**, with 3-methoxy-4-hydroxyphenyl ring, that shows 91% of inhibition at 9 μM and 51% at 900 nM.

Table 2. Inhibition of *EeAChE* and *eqBChE* activities by pyridine diamine derivatives **23-33**.

Cmp	R	n	% inhibition vs <i>EeAChE</i> ± SD ^a		% inhibition vs <i>eqBChE</i> ± SD ^a		
			[I] 9 μM	[I] 900 nM	[I] 9 μM	[I] 900 nM	[I] 90 nM
23		3	53.5 ± 1.4	10.3 ± 0.8	56.5 ± 3.0	5.0 ± 5.8	nd ^b
24		3	18.2 ± 3.5	nd ^b	56.4 ± 1.6	12.1 ± 4.6	nd ^b
25		4	73.3 ± 0.1	23.1 ± 5.7	71.6 ± 2.1	16.6 ± 6.3	nd ^b
26		4	23.5 ± 2.2	nd ^b	76.8 ± 0.5	17.0 ± 2.7	nd ^b
27		4	27.7 ± 4.7	nd ^b	73.2 ± 3.6	17.7 ± 5.2	nd ^b
28		4	58.6 ± 1.1	9.0 ± 1.6	74.3 ± 1.4	24.2 ± 3.3	nd ^b
29		4	30.9 ± 1.1	nd ^b	68.9 ± 4.1	19.0 ± 2.5	nd ^b
30		4	61.8 ± 1.9	17.3 ± 0.6	90.9 ± 0.6	51.2 ± 3.1	15.6 ± 6.1
31		4	42.2 ± 2.2	nd ^b	56.0 ± 3.8	19.1 ± 2.2	nd ^b
32		4	63.9 ± 2.2	23.9 ± 1.5	59.8 ± 1.5	11.5 ± 2.9	nd ^b

33		4	40.6 ± 4.1	6.2 ± 1.1	68.3 ± 2.9	13.0 ± 0.7	nd ^b
	Tacrine	100	97.6 ± 0.1	100	99.7 ± 0.3	96.1 ± 0.2	

^a Data are the average of three replicates; ^b nd stands for not determined

For a selection of compounds, among the most potent as inhibitors of *EeAChE* and/or *eqBChE*, the inhibition constant (K_i) and the corresponding inhibition mechanism were determined according to Dixon's method,²⁶ reporting in graph the reciprocal of the hydrolysis rate versus the inhibitor concentrations at a fixed concentration of substrate. The recorded data were analyzed with the enzyme kinetic module of SigmaPlot, in order to find the best fitting model of inhibition, using the linear regression analysis. The reference kinetic models used in the regression analysis were: competitive, non-competitive, uncompetitive and mixed. Each determination was repeated five times and incorrect values were discarded to reduce the standard deviation within the limit of 5%. In this way, the regression lines obtained have a linear regression coefficient (R^2) higher than 0.95. The Dixon's plots of all tested compound are reported in the supporting information (Figure S1-S12).

The tested compounds revealed mixed or uncompetitive inhibition mechanism towards *EeAChE* and *eqBChE*, with K_i according to the order of low micromolar or nanomolar (Table 3). The mixed inhibition mechanism might suggest an interaction of the compound with both CAS and PAS of the enzyme and a possible involvement in the inhibition of A β plaques formation induced by AChE.

The pyrimidine amine compounds are more potent on *EeAChE* than the pyridine analogous, as confirmed by K_i values of **9** and **13** (pyrimidine derivatives with phenyl ring on one side of the aliphatic chain, respectively with five or six methylene), compared to K_i values of **23** and **25** (pyridine derivatives with phenyl ring on one side of the aliphatic chain, respectively with

five or six methylene). All the compounds tested on *EeAChE* show a mixed inhibition mechanism, with the exception of **19**, that acts with an uncompetitive mechanism. The most potent inhibitors of *EeAChE* are the compounds **9** and **13**, with K_i values of 312 ± 108 nM and 426 ± 132 nM respectively.

Generally, pyridine amine derivatives are more potent on *eqBChE* than the corresponding pyrimidine derivatives. All the compounds tested on *eqBChE* show a mixed inhibition mechanism. The compound **22** (pyrimidine derivatives with indole group on one side of the aliphatic chain) is the most potent inhibitor of *eqBChE*, with K_i equal to 99 ± 71 nM.

Table 3. Inhibition constants (K_i) and inhibition mechanisms on *EeAChE* and *eqBChE*.

Cmp	<i>EeAChE</i>			Cmp	<i>eqBChE</i>		
	Mechanism	$K_i \pm SD$ (μ M)	R^2		Mechanism	$K_i \pm SD$ (μ M)	R^2
9	mixed	0.312 ± 0.108	0.982	18	mixed	3.034 ± 0.604	0.986
13	mixed	0.426 ± 0.132	0.991	22	mixed	0.099 ± 0.071	0.990
19	uncomp.	0.509 ± 0.018	0.992	25	mixed	2.373 ± 0.304	0.992
23	mixed	0.743 ± 0.316	0.983	26	mixed	3.465 ± 1.480	0.950
25	mixed	0.995 ± 0.374	0.988	28	mixed	3.434 ± 0.701	0.988
28	mixed	1.323 ± 0.622	0.990	30	mixed	1.105 ± 0.189	0.983

For the pyrimidine amine derivative **20**, with 2,3-dihydroxyphenyl ring on one side of the aliphatic chain, it was necessary to determine the IC_{50} on *EeAChE* (concentration of inhibitor required to inhibit 50% of the enzyme), instead of the K_i , due to the instability of this molecule in aqueous solution for the time required for K_i determination. The IC_{50} value was obtained plotting the percentages of inhibition towards *EeAChE* versus the concentration of inhibitor expressed in logarithmic scale, at fixed substrate concentration. The recorded data were

analyzed with the enzyme kinetic module of SigmaPlot. All measurements were replicated three times and the IC₅₀ value obtained was confirmed by repeating the experiment twice. For the compound **20** the IC₅₀ on *EeAChE* is 622 ± 30 nM, as shown in Table 4. The IC₅₀ plot of the tested compound is reported in the supporting information (Figure S13).

Table 4. IC₅₀ (concentration of inhibitor required to inhibit 50% of the enzyme) on *EeAChE* for compound **20** and on both ChEs for tacrine and donepezil, used reference standard.

Cmp	<i>EeAChE</i>	<i>eqBChE</i>
	IC ₅₀ ± SE (nM)	IC ₅₀ ± SE (nM)
20	621.9 ± 29.5	nd ^a
Tacrine	41.0 ± 4.9	3.7 ± 0.5
Donepezil	16.2 ± 1.8	1727 ± 300

^a nd stands for not determined.

Molecular docking studies

Molecular modelling analyses were performed to provide structural insights on the binding mode of the investigated compounds into *hAChE* and *hBChE* catalytic pocket. For the current study, the x-ray crystallographic structures of the *hAChE* in complex to donepezil (PDB code: 4EY7)¹³ and the *hBChE* in complex to the naphthamide derivative (PDB code: 5NN0)²⁷ were used. As there is no crystal structure of *eqBChE* in the protein data bank (PDB), *hBChE* was used for the computational study. Indeed, the sequence of *eqBChE* derived from Uniprot Database shares 90% sequence identity with that of the adopted *hBChE* (PDB code: 5NN0), above all comparing residues of the binding site (Figure S14). Regarding AChE, even if the apo-crystal structures of *EeAChE* are present in PDB, they cannot be considered as good quality models. After alignment of *EeAChE* (PDB code: 1C2O) with the adopted *hAChE*

structure (PDB code: 4EY7), 94.7% of the identity of the aligned sequences within a range of 7 Å from the binding site is obtained (Figure S15). According to a previous work²³ and the criteria for the identification of reliable complexes reported in the literature,²⁸ the selected models were considered as a good starting point for *in silico* investigation.

Our docking protocol was validated by docking co-crystallized ligands into the binding site. Root Mean Square Deviation (RMSD) values between the native pose of *hAChE* and *hBChE* ligands and the related best re-docked conformations were found to be 0.12 Å and 0.96 Å, respectively, thus revealing the reliability of docking protocol (Figure S16). According with previously published studies,^{23, 29} no linear correlation between docking score and the experimental data is expected (Table S1). Nevertheless, the obtained docking poses for the analysed compounds were comparable with the binding mode of donepezil into AChE (Figure S17). It is widely known that donepezil is a dual binding site inhibitor, i.e., engaging simultaneously π -cation and π - π interactions with Trp86 and Trp286 of the CAS and the PAS, respectively. Moreover, the ketone group of the indanone ring of donepezil formed a hydrogen bond with Phe295 of the mid-gorge binding site. In detail, CAS region is characterized by Trp86, Tyr119, Tyr124, Tyr133, Glu202, Ser203, Trp439, His447, Tyr449, and PAS region is composed of Tyr72, Asp74, Thr75, Trp286, Leu289, Tyr341, and Val365 residues. The mid-gorge pocket of *hAChE* consists of Leu76, Phe295, Arg296, Phe297, Tyr337, Phe338, and it is about 20 Å deep by an average of 13 Å wide.

Particularly, it is showed that, regardless of the aliphatic chain length, the protonated amine group interacted with Trp86 of the anionic site of CAS for all the docked compounds, except for compound **29**, which interacted with Tyr341 and Tyr337 of the mid-gorge site.

Both 2-amino-pyrimidinic or 2-amino-pyridinic moiety exhibited hydrogen bonds with Phe295 and Arg296 in the mid-gorge pocket, except for compound **13**, whose pyrimidine cycle was more exposed to the solvent. The introduction of the other aromatic ring contributed to the

stabilization of the compounds in the CAS region. Molecular recognition studies revealed the major binding interactions between our most potent inhibitors with *hAChE* (compounds **9**, **13**, **19** and **20**) (Figure 2) and *hBChE* (compounds **22** and **30**) (Figure 3).

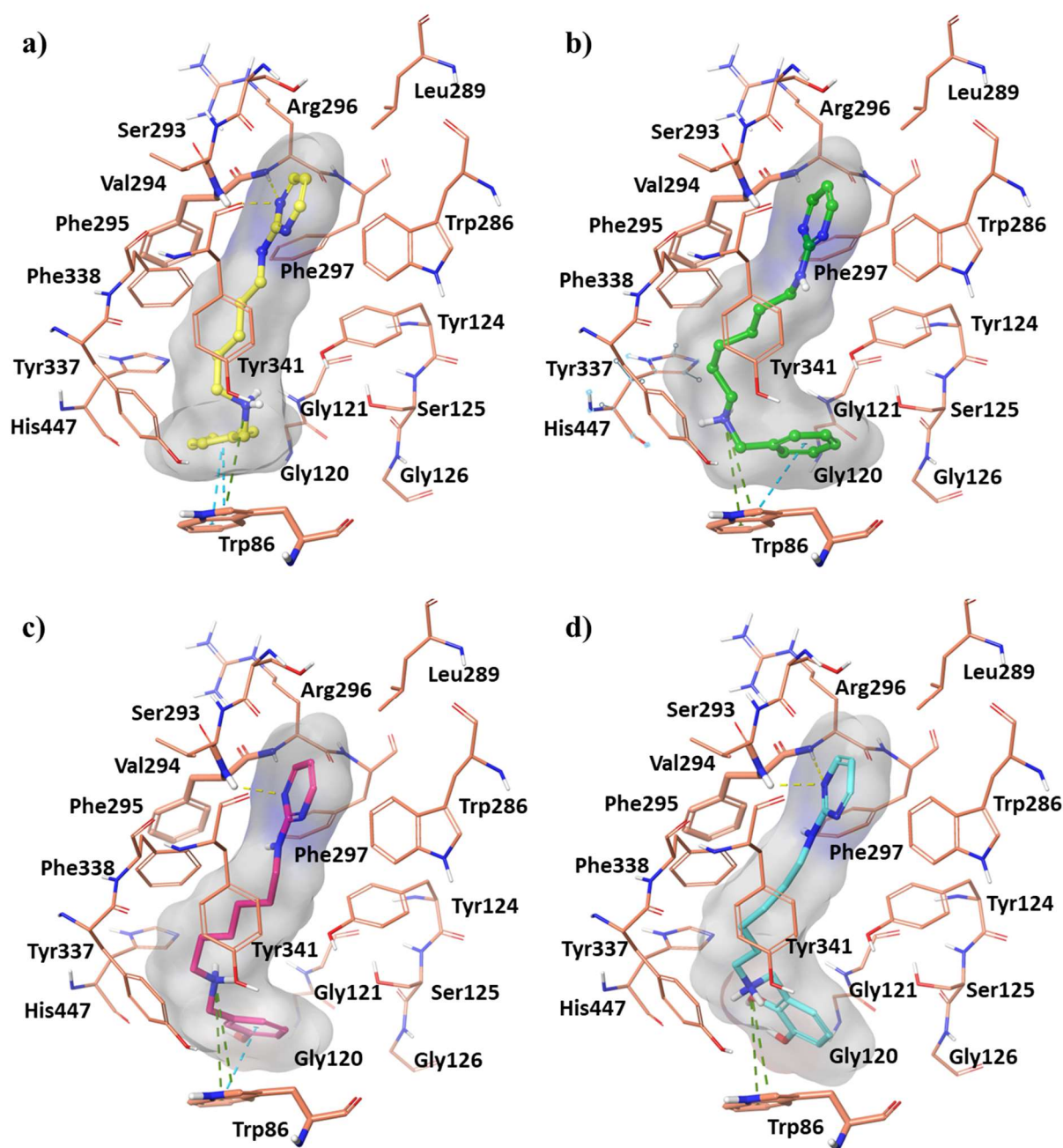


Figure 2. Best docking pose of compounds: (a) **9**, (b) **13**, (c) **19** and (d) **20** into *hAChE* active site shown as wire representation. Most relevant interacting residues are displayed as thin salmon tubes. Compounds **9**, **13**, **19**, and **20** are illustrated in yellow, green, pink and blue carbon ball and stick representation, respectively. Hydrogen bonds, π - π interactions, and π -cation contacts are respectively represented in yellow, blue, and green dotted lines.

Compound **9** pyrimidine group formed two hydrogen bonds with Phe295 and Arg296 (Figure 2a). The phenyl ring also created a π - π stacking interaction with Trp86, while the protonated amine contributed to the accommodation at the CAS and PAS sites by means of a π -cation with Trp86 and a salt bridge with Asp74, respectively. The aliphatic extension of one methylene unit in compound **13** (Figure 2b) induced a destabilization of the hydrogen bonds between the pyrimidine portion and mid-gorge amino-acids. Conversely, this orientation allowed a π -cation interaction between the protonated amine group and the indole ring of Trp86, with the loss of the interaction with Asp74 observed for compound **9**, still maintaining the π - π interaction between the phenyl group and Trp86.

Concerning compounds **19** and **20** (Figure 2c and 2d), they showed very similar docking poses orientating the protonated amine group towards Trp86 and interacting with Tyr133 and Glu202 through two and three hydrogen bonds with phenolic and catecholic group, respectively.

As regards *hBChE*, all the investigated compounds were able to accommodate into the binding cavity with a lower binding affinity with respect to that of *hAChE*, due to the presence of more hydrophilic and charged residues in the PAS and mid-gorge site.

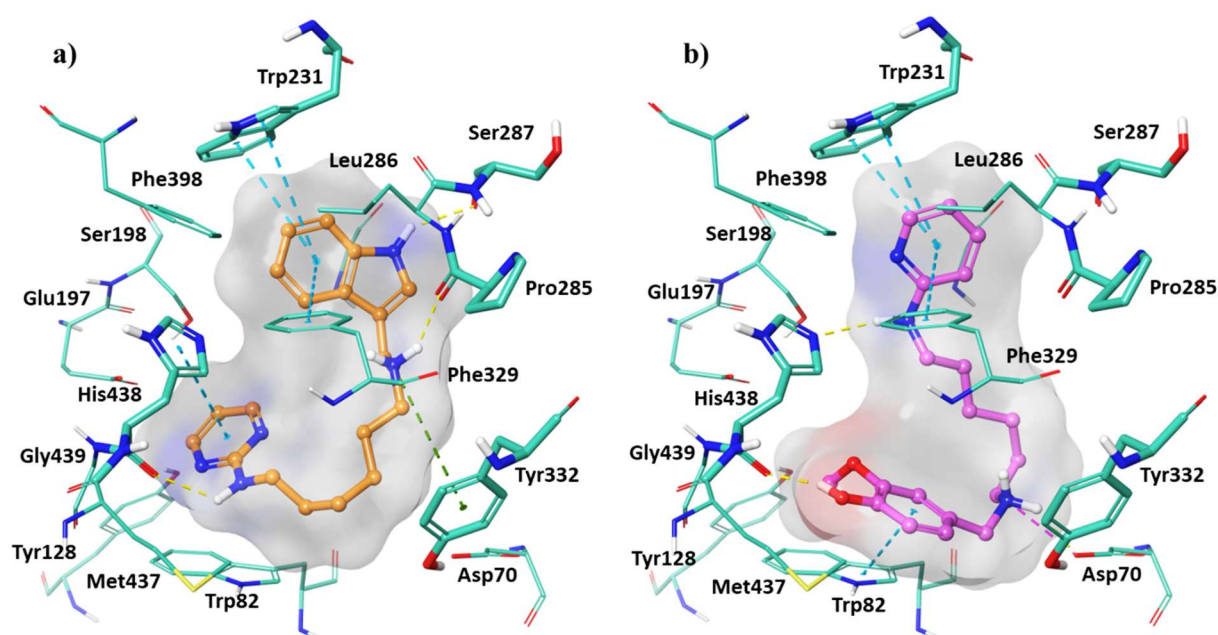


Figure 3. Best docking pose of compounds: (a) **22** and (b) **30** into *h*BChE active site showed as wire representation. The most relevant interacting residues are displayed as thin light green tubes. Compound **22** and **30** are illustrated in orange and pink carbon ball and stick representation, respectively. Hydrogen bonds, π - π interactions and π -cation contacts are respectively represented in yellow, blue, and green dotted lines.

In detail, the pyrimidine moiety of compound **22** (Figure 3a) created a π - π interaction with His438, and this residue also engaged a hydrogen bond with the amine group. Furthermore, a π -cation and a hydrogen bond were formed between the ligand protonated amine and Tyr332, and Pro285, respectively. The indole moiety pointed to Trp231 in CAS and Phe329 in mid-gorge regions, providing also a hydrogen bond with Ser287. Compound **30** (Figure 3b) showed a different docking pose orientating the pyridine towards Trp231 and Phe329. It interacted with His438 by means of the hydroxyphenyl at position 4, while the amine group bound to the pyridine. Its 3-methoxy-4-hydroxyphenyl ring was able to engage a π - π stacking interaction with Trp82. With Asp70, belonging to the PAS region, that phenolic moiety established one hydrogen bond and the protonated amine group an additional salt-bridge.

Molecular dynamics (MD) studies

The best docked poses of compounds **9**, **13**, **19**, and **20** into binding pockets of *hAChE* and compounds **22** and **30** into that of *hBChE* were submitted to 250 ns of molecular dynamics (MDs) simulations. The results of MDs were investigated in terms of stability of the complexes and conformational flexibility of *hChEs* in presence of the promising inhibitors by monitoring the single contributions of hydrophobic, water bridges and hydrogen bonding interactions.

The stability of the *hChEs* complexes trajectories can be monitored by the RMSD of the protein's backbone atoms from its initial to final conformation over an MDs time of 250 ns (Figure 4). As shown, the RMSD plot indicated that all compounds in complex to *hAChE* (Figure 4a) and *hBChE* (Figure 4b) maintained overall stability during the whole MDs, thus ensuring a good equilibrium for the systems. Particularly, compounds **9**, **13**, and **20** in complex to *hAChE* were associated with increased conformational stability with RMSD average values of 1.89, 2.25, and 2.04 Å, respectively, in comparison to compound **19** (2.60 Å). As to compounds **22** and **30** in complex to *hBChE*, a similar stability trend was observed, resulting in very low fluctuations and RMSD average values of 2.13 and 2.06 Å, respectively.

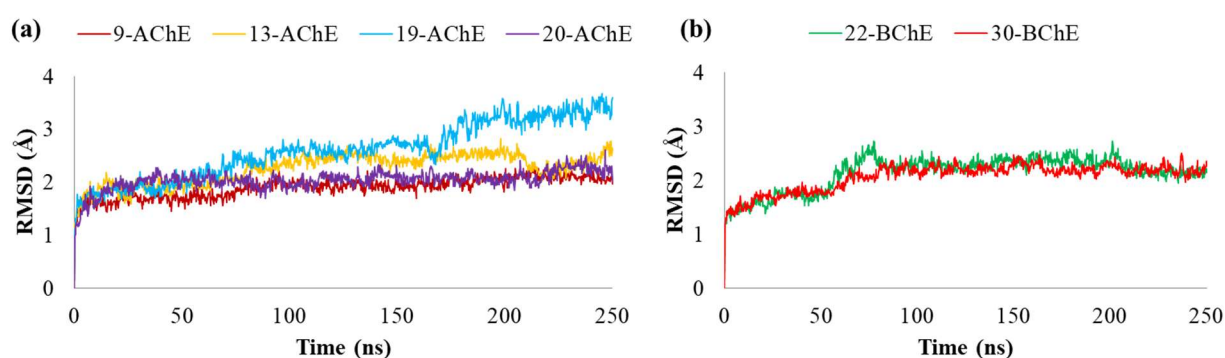


Figure 4. (a) RMSD of compounds **9**, **13**, **19** and **20** and backbone atoms of *hAChE*. (b) RMSD of compounds **22** and **30** and backbone atoms of *hBChE*.

Compound **9** protonated amine group interacted mainly with the amino acids of both CAS and PAS regions of the *hAChE* pocket. Indeed, Asp74, Trp86, His447, and Tyr337 for 46%,

53%, 38%, and 46% of the MDs time were engaged respectively. The pyrimidine ring also formed a π - π interaction with Tyr341 (35%) of the mid-gorge site. Carefully looking at compound **13** accommodation into *hAChE* pocket during MD, it can be observed that the protonated amine group participated in major interactions with Trp86 (24%), Glu202 (96%), His447 (17%), Gly448 (97%). Tyr124 also provided a significant hydrogen bond in overall simulation (96%), while Phe297 and Tyr341 engaged a π - π stacking interactions with pyrimidine moiety, and one of its nitrogen atoms displayed two water bridges, with Phe295 (42%) and Arg296 (21%), located at the mid-gorge. Finally, the phenyl ring was surrounded by the aromatic residues of the CAS region through hydrophobic interaction with Trp86 and Tyr449 for 35% and 41% of MDs time. The hydroxyphenyl in compound **19** and 2,3-dihydroxyphenyl ring in compound **20** were inserted into the CAS region, interacting with Tyr133 for 84%, and with Glu202 for 67% of the MD time, respectively. Also, the 2,3-dihydroxyphenyl ring formed a strong π - π stacking interaction with Trp86 during the whole trajectory. The pyrimidine moiety formed a water-bridge with Phe295 for 33% and 58% of MDs for compounds **19** and **20**, respectively. The last one was also stabilized by the hydrogen bond between the nitrogen atom of the pyrimidine ring and Tyr124 at the CAS site (62%). The protonated nitrogen of compound **19** exhibited a noticeable 96% π -cation with Trp86, 89% hydrogen bond with Glu202, 36% water-bridge interaction with His447 residue. While, in compound **20**, the positively charged group displayed long persistency in the interaction with Asp74 (69%), Trp86 (66%), and Ser125 (86%).

Analyzing the main interactions of compounds **22** and **30** during MDs, it was possible to observe the effect of the different orientation of the former *versus* the latter in *hBChE*.

Indeed, the indole moiety of the compound **22** engaged hydrophobic interactions with Trp231 (45%) and Phe329 (28%), a hydrogen bond with Ser287 (44%), and a water bridge with Pro285 residue in CAS and mid-gorge pockets. The flexibility of the ligand allowed to

orient the protonated amine group towards the catalytic region forming a hydrogen bond with His438, a water bridge with Glu197, and a salt bridge with Trp82 at the CAS site. The insertion of pyrimidine contributed to the stabilization of *h*BChE into the CAS region due to the interaction with Trp82, Tyr440, and Trp430. Instead, the opposite orientation of compound **30** favoured the interaction of the pyridine ring in the π - π stacking interactions with Trp231 and Phe329 for 50% and 69% of the time of the simulation. This also directed the amino group towards Ser198 (20%) of the catalytic region and the 3-methoxy-4-hydroxyphenyl ring towards His438 (37%). Such rearrangement led the protonated amine group anchoring to Asp70 (10%) and Trp82 (35%) at PAS and CAS sites, respectively.

In summary, MDs results reveal the role of pyrimidine ring, protonated amine group, and the substituted aromatic moiety of the pyrimidine derivatives in occupying CAS, PAS, and mid-gorge cavities, thus suggesting their promising role as dual binding site inhibitors.

The protonated amine group inserted into linear alkyl chains of five or six methylene units is one of the crucial pharmacophore features for ChEs inhibition and it mainly establishes strong interactions with the catalytic site and PAS region.

The pyrimidine diamine scaffold bearing indole moiety and 3-methoxy-4-hydroxyphenyl ring drives the selectivity of the molecule toward BChE inhibition.

Instead, phenolic and catecholic rings represent high selectivity for AChE inhibition, strongly supported by interaction with Tyr133 and Glu202 of AChE binding pocket.

Finally, the phenyl ring of compounds **9** and **13**, which differ only for the length of the alkyl chain, is well stabilized into the bottom of the gorge.

Chelation studies

For a selection of compounds, among the most potent as inhibitors of *Ee*AChE and/or *eq*BChE, in order to define their possible multitarget profile, metal chelation studies were

performed by using UV-Vis spectrophotometric analysis, a method widely used for investigating chelates.^{30,31}

The chelating ability of pyrimidine and pyridine compounds **9**, **13**, **18**, **19**, **20**, **25**, **28**, **30** on bio-metals Fe^{3+} , Cu^{2+} and Zn^{2+} was evaluated. Initially the UV-Vis spectrum of the ligand was recorded and compared with the spectra obtained by adding an excess of metal to the ligand solution, maintaining the same concentration of ligand (ligand/metal ratio 1:3, 1:5 or 1:10). The variation of the UV-Vis spectrum of the ligand in presence of metal ions is indicative of the formation of the complex. Based on this, it has been observed that all the tested pyrimidine and pyridine derivatives have the ability to chelate Fe^{3+} and Cu^{2+} ions, while only the compound **20** shows chelating capacity also on Zn^{2+} . Based on these results it can be stated that the chelating activity of these compounds is due to the presence of two adjacent nitrogen atoms in the 2-aminopyrimidine or 2-aminopyridine moiety. For the derivatives **18-20** and **30** it is also possible that the phenolic portion participates in the formation of the complex. In particular, the catechol ring in **20** could be responsible for the ability of this molecule to chelate also Zn^{2+} .

UV-Vis titrations of these compounds were carried out with the metal ions with which they form complexes, recording first the UV-Vis spectrum of the ligand and then the spectra obtained by mixing solutions of ligand and metal according to increasing metal/ligand molar ratios (Figure 5a).

The stoichiometries of metal-ligand complexes were determined through the Job's method.^{32,33} In the Job's plot the values of ΔA , measured at the wavelengths where evident absorbance variations were observed in the titration spectra, are in ordinate and the mole fractions of the ligand are in abscissa. The mole fraction X, that causes the maximum variation of absorbance, is extracted from the graph and then the value of the coefficient n, which corresponds to the number of ligand molecules per cation, is obtained (Figure 5b). The UV-Vis titrations spectra

and the Job's plots of all the tested compounds are reported in the supporting information (Figure S18-S46), while the data extrapolated from the Job's plots are summarized in Table 5.

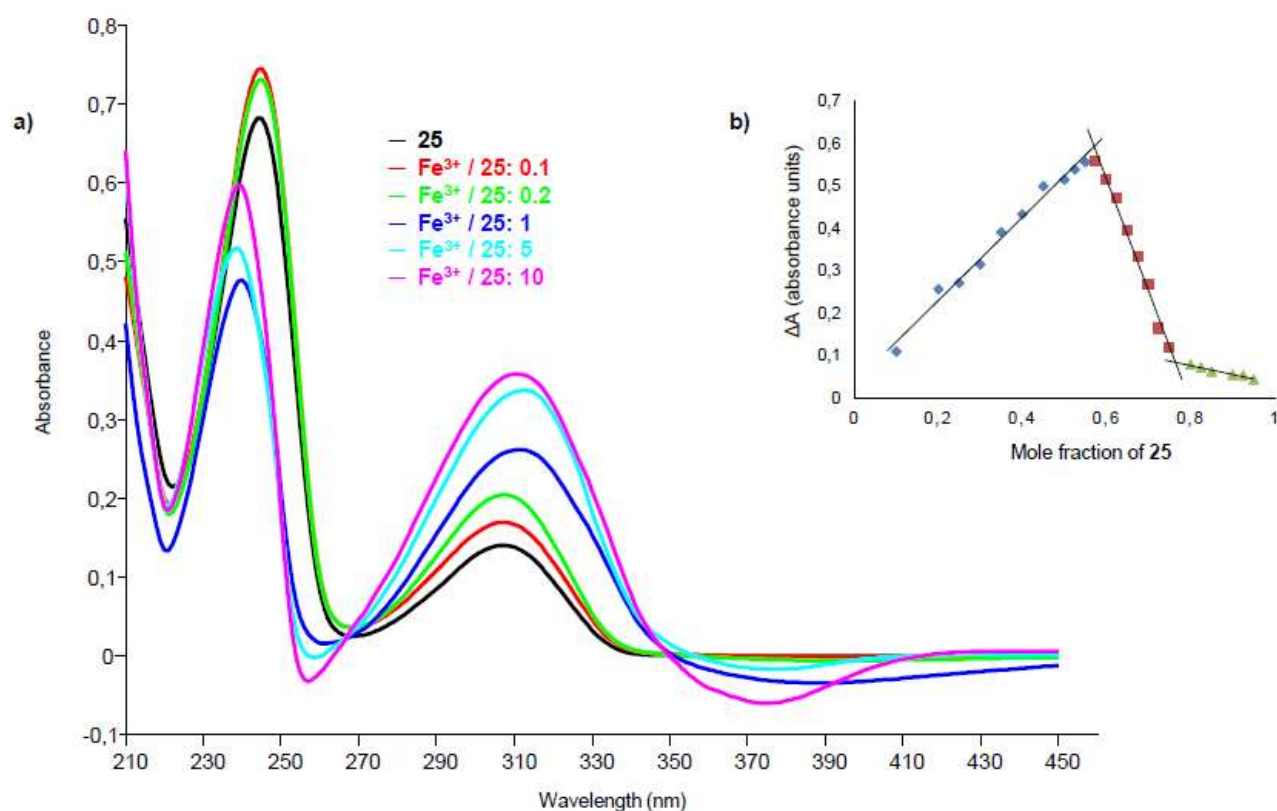


Figure 5. (a) UV-Vis titration of ligand **25** with Fe^{3+} . The greatest variations in spectra with increasing amount of metal are observed at 251 and 374 nm, with a reduction of absorbance, and at 318 nm, with an increase of absorbance. There are two isosbestic points at 270 and 350 nm. (b) Job's plot of compound **25** in presence of Fe^{3+} : variation of the absorbance (ΔA) at the wavelength of 318 nm, in ordinate, versus the mole fraction of **25**, in abscissa. X_1 (mole fraction that causes the maximum variation of absorbance) = 0.57; $X_2 = 0.77$; n_1 (number of ligand molecules per cation) = 1; $n_2 = 3$.

Table 5. Job's plot data for the tested compounds in presence of Fe^{3+} and Cu^{2+} . The table shows the wavelength values (λ) in which the absorbance variation was measured, the molar ratios (X) that cause the maximum variation of absorbance and the coordination values (n) which correspond to the number of ligand molecules per cation.

Fe^{3+}	Cu^{2+}

Cmp	_____			_____		
	λ (nm)	X	n	λ (nm)	X	n
18	375	0.69	2	330	0.70	2
19	375	0.68	2	330	0.51	1
20	370	X ₁ = 0.53 X ₂ = 0.80	n ₁ = 1 n ₂ = 4	330	0.53	1
25	318	X ₁ = 0.57 X ₂ = 0.77	n ₁ = 1 n ₂ = 3	330	0.44	1
28	316	X ₁ = 0.53 X ₂ = 0.74	n ₁ = 1 n ₂ = 3	330	0.53	1
30	310	X ₁ = 0.53 X ₂ = 0.74	n ₁ = 1 n ₂ = 3	312	0.50	1

Antioxidant activity

In order to characterize multitarget compounds, antioxidant activity assays were carried out on **18**, **19**, **20** and **30**, since they are the most potent ChEs inhibitors among phenolic derivatives, they exert chelating activity on metal ions involved in Alzheimer's disease and they have a structure that could justify an antioxidant activity.

The antioxidant activity assays were carried out according to 2,2-diphenyl-1-picrylhydrazyl (DPPH) spectrophotometric method.³⁴ Initially, to assess whether the compounds had antioxidant activity and to define the time required by each antioxidant to reach the steady state, the reduction in absorbance over time at 515 nm of a solution of DPPH mixed with the tested compound was recorded, until reaching the plateau. From these measurements compound **19** did not show significant ability to interact with DPPH, since reduction of the absorbance over time was not observed; otherwise compounds **18**, **20** and **30** possess antioxidant activity, as a reduction in absorbance over time, until reaching the plateau (in 1 minute for **20**, 90 minutes for **18** and **30**), was observed. Subsequently the EC₅₀, defined as the

ratio of moles of antioxidant which reduce by 50% the initial concentration of DPPH to initial moles of DPPH, was determined for compounds **18**, **20** and **30**. The value of EC₅₀ can be extrapolated by plotting the percentage of residual DPPH at the steady state as a function of molar ratio of antioxidant to initial DPPH.

Based on the obtained results, reported in Table 6, the more efficient antioxidant, even better than ascorbic acid, used as positive control, is the catechol derivative **20**, both for the high reaction rate with DPPH and for the EC₅₀ value, equal to 0.1366 ± 0.0060 . The compounds **18** and **30**, having the 3-methoxy-4-hydroxyphenyl ring, show antioxidant capacity lower than **20** and comparable to each other, with EC₅₀ respectively equal to 0.5997 ± 0.0940 and 0.6419 ± 0.0730 .

Table 6. EC₅₀ values and times for reaching the plateau for the tested compounds.

Compound	EC ₅₀ ± SD ^a	Reaction time (min)
18	0.5997 ± 0.0940	90
20	0.1366 ± 0.0060	1
30	0.6419 ± 0.0730	90
Ascorbic acid	0.2650 ± 0.0070	2

^a Data are the average of three independent assays.

Inhibition of amyloid and Tau aggregation

For the most potent ChEs inhibitors the direct anti-amyloid aggregation activity against Aβ₄₂ and Tau aggregation was evaluated. The anti-aggregating effect of the tested compounds was monitored by a cell-based assay in intact *Escherichia coli* cells that overexpress either Aβ₄₂ peptide or Tau protein, which upon over-expression form insoluble inclusion bodies that were stained with thioflavin-S, an amyloid specific dye.³⁵ The percentages of inhibition towards Aβ₄₂ and Tau aggregation were determined at inhibitor concentration of 100 μM and the

obtained results are reported in Table 7. Low percentages of inhibition were found both on A β ₄₂ (up to 22%) and on Tau (up to 17%), so these compounds have weak anti-aggregating activity. The pyridine derivative **28** is the best inhibitor of aggregation of both A β ₄₂ and Tau, while the pyrimidine **13** showed similar percentage of inhibition on A β ₄₂ aggregation, but lower towards Tau.

Table 7. Inhibition of A β ₄₂ aggregation and Tau aggregation by the tested compounds.

Cmp	A β ₄₂ aggregation		Tau aggregation	
	% inhibition [I] = 100 μ M	SEM ^a	% inhibition [I] = 100 μ M	SEM ^a
9	5.8	1.6	2.6	6.7
13	21.0	4.2	12.6	6.6
18	1.7	2.1	1.0	4.1
19	16.7	2.7	9.9	3.9
20	7.2	2.4	4.6	1.0
22	9.7	1.8	6.8	6.1
23	10.4	3.9	7.0	4.2
25	16.8	2.9	6.7	2.9
26	7.3	3.7	7.3	4.8
28	22.3	3.3	17.0	6.4
30	13.6	5.3	12.8	2.7

^a A minimum of 5 independent assays (with three replicates for assay) were performed for each tested compound. More assays were performed to obtain a SEM < 5% with a maximum of 10 independent assays.

Computation of physicochemical descriptors and ADME parameters

Physicochemical descriptors and ADME parameters of the most interesting compounds, by virtue of their inhibitory activity towards ChEs, as well as chelating and antioxidant ability, were predicted by means of SwissADME public server³⁶ and the obtained data are reported in Table 8. All the studied compounds fit the Lipinski's rule of five (MW \leq 500; MLogP \leq 4.15;

H bond acceptor ≤ 10 ; H bond donor ≤ 5).³⁷ They should be soluble or moderately soluble in water. They should have high gastrointestinal absorption after oral administration. Worthily, these compounds should be BBB accessible, with the exception of **18** and **20**.

Table 8. Predicted physicochemical properties and ADME parameters: Molecular Weight (MW); number H-bond acceptors (H-b acc); number H-bond donors (H-b don); number of heavy atoms (heavy atoms); number rotatable bonds (rot bonds); Topological Polar Surface Area in \AA^2 (TPSA); octanol/water partition coefficient (MLogP); water solubility (LogS ESOL); water solubility class (Sol class); gastrointestinal absorption (GI); Blood-Brain Barrier permeation (BBB); number of Lipinski's rule of five violations (Lipinski viol). Data was obtained by SwissADME public server.³⁶

Cmp	MW	H-b acc	H-b don	Heavy atoms	Rot bonds	TPSA	MLogP	LogS ESOL	Sol class	GI	BBB	Lipinski viol
9	270.37	3	2	20	9	49.84	1.88	-3.04	Soluble	High	Yes	0
13	284.40	3	2	21	10	49.84	2.12	-3.26	Soluble	High	Yes	0
18	330.42	5	3	24	11	79.30	1.25	-3.19	Soluble	High	No	0
19	300.40	4	3	22	10	70.07	1.56	-3.12	Soluble	High	Yes	0
20	316.40	5	4	23	10	90.30	1.01	-3.32	Soluble	High	No	0
22	323.44	3	3	24	10	65.63	1.87	-3.63	Soluble	High	Yes	0
23	269.38	2	2	20	9	36.95	2.56	-3.45	Soluble	High	Yes	0
25	283.41	2	2	21	10	36.95	2.80	-3.67	Soluble	High	Yes	0
26	362.31	2	2	22	10	36.95	3.42	-4.57	Moderately soluble	High	Yes	0
28	313.44	3	2	23	11	46.18	2.45	-3.73	Soluble	High	Yes	0
30	329.44	4	3	24	11	66.41	1.89	-3.59	Soluble	High	Yes	0

Furthermore, all synthesized final compounds were screened using *in silico* public tools, specified in the experimental section, and were not found to be Pan Assay INterference

compounds (PAINS),³⁸ except for **20** and **32**. Nevertheless, the activities of these compounds are in line with those of the other pyrimidine and pyridine molecules studied and they can be framed in logical SAR, as previously discussed. Moreover, compound **20** showed strongly different activity towards the related targets *EeAChE* and *eqBChE* (percentages of inhibitions at 9 μM equal to 90.5 ± 0.5 and 17.1 ± 1.6 , respectively, Table 1) and it was not cytotoxic at concentrations up to 10 μM , as reported in the subsequent section. Overall, these evidences suggested that these molecules do not act *via* a PAINS mechanism.

Cytotoxicity assays

A selection of the most active inhibitors of *EeAChE* and *eqBChE* (**9**, **13**, **19**, **20**, **22**, **23**, **25**, **26** and **28**) were tested to evaluate the cytotoxic effects on U-87 MG Cell Line from human brain (glioblastoma astrocytoma) at concentration ranging from 1 to 50 μM . The obtained data, represented in the histogram of Figure 6, suggest that the tested compounds are characterized by low toxicity towards the studied cells, in particular at concentrations up to 10 μM . In general, the pyrimidine derivatives appear to be less cytotoxic than pyridine derivatives, as evidenced by the comparison of the pyrimidines **9** and **13** with the corresponding pyridines **23** and **25**. The pyridines tested showed a very similar toxicity profile, with the exception of compound **23** (having the spacer chain with five methylene), which at concentrations of 1 μM and 5 μM showed a lower cytotoxic effect. Also, among pyrimidine derivatives, the compound **9**, with five methylene units, exerted a minor effect on cell viability than the corresponding compound **13**, with six methylene units. Moreover, among pyrimidine derivatives the compound **22**, with an indole group on one side of the aliphatic chain, showed a more pronounced cytotoxic effect, with a toxicity profile similar to the tested pyridines.

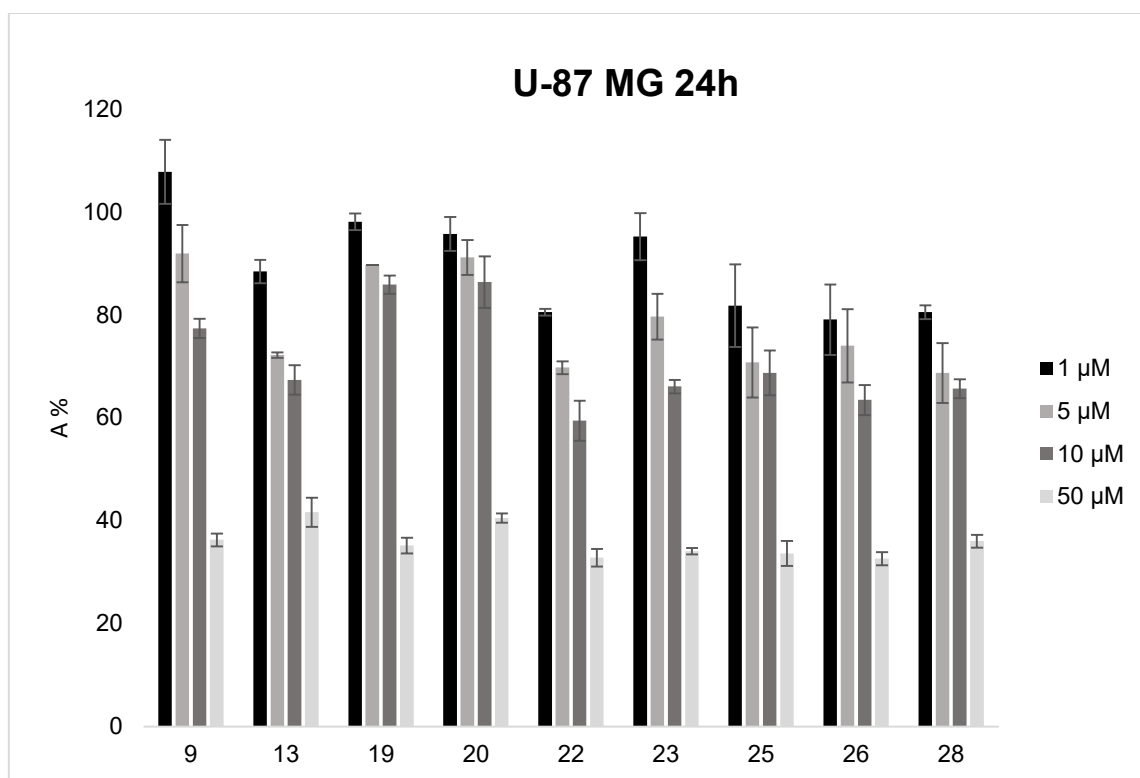


Figure 6. Cell viability assay of U-87 MG cells in presence of increasing concentration of studied compounds, evaluated using the MTT method. Data represent the absorbance % (\pm SD) relative to untreated cells in the same experiment and standardized to 100%. All data points were performed in triplicate and at least three independent experiments.

Conclusions

Series of pyrimidine and pyridine derivatives were designed as potential multifunctional compounds for AD, whose purpose could be to restore the cholinergic tone by inhibition of ChEs, attenuate the dyshomeostasis of the metals mainly involved in the pathology, reduce the oxidative stress and contrast the toxicity and deposition of the A β peptide. These compounds contain two π systems, one of which is represented by a 2-aminopyrimidine or 2-aminopyridine moiety, connected to a small aromatic group by a flexible amino-alkyl linker.

On the synthesized compounds enzymatic inhibition studies were carried out towards *EeAChE* and *eqBChE*. The initial determination of the percentages of inhibition at concentration equal to 9 – 0.09 μ M led to the identification of the most potent inhibitors. For a selection of these compounds the K_i was determined, obtaining values in the range 0.312 –

1.323 μM vs *EeAChE* and 0.099 – 3.465 μM vs *eqBChE*. All the tested compounds result mixed inhibitors of ChEs, with the only exception of **19**, that acts with an uncompetitive mechanism towards *EeAChE*. The uncompetitive inhibitors might interact with allosteric modulation site such as PAS, while mixed inhibitors interact simultaneously with both CAS and PAS of the enzyme; these evidences may suggest that these compounds could interfere with aggregation of A β plaques induced by AChE through interactions with PAS.

In general, the pyrimidine amine compounds are more potent on *EeAChE* than the pyridine analogous. On the contrary, pyridine amine derivatives are more potent on *eqBChE* than the corresponding pyrimidine derivatives. The greater inhibitory potency towards *EeAChE* is showed by compounds **9** ($K_i = 0.312 \pm 0.108 \mu\text{M}$) and **13** ($K_i = 0.426 \pm 0.132 \mu\text{M}$), both having the unsubstituted phenyl ring on one side of the aliphatic chain; indeed, modifications of the phenyl group, both adding substituents and changing the type of aromatic ring, reduce the inhibition activity towards *EeAChE*. Differently, the most potent inhibitor of *eqBChE* is **22** ($K_i = 0.099 \pm 0.071 \mu\text{M}$), the pyrimidine derivatives with indole ring on one side of the aliphatic chain.

In silico analyses highlighted that the protonated amine group inserted into linear alkyl chain is the pivotal pharmacophore feature for ChEs inhibition, due to its strong interaction with the catalytic site and PAS region. Moreover, the pyrimidine diamine scaffold, bearing the indole moiety and 3-methoxy-4-hydroxyphenyl ring, resulted to drive the selectivity of the molecule toward BChE inhibition. On the other hand, phenolic and catecholic rings were responsible for the AChE inhibition selectivity, strongly supported by interaction with Tyr133 and Glu202 of this enzymatic binding pocket. Additionally, the phenyl ring of compounds **9** and **13**, which differ only for the length of the alkyl chain, is well stabilized into the bottom of the gorge. Based on the computational results, the involvement of pyrimidine ring, protonated amine

group, and the substituted aromatic moiety of these derivatives in occupying CAS, PAS, and mid-gorge cavities, suggested their potential role as dual binding site inhibitors.

Metal chelation studies revealed that all the tested compounds have the ability to chelate Fe^{3+} and Cu^{2+} ions; this chelating activity can be attributed to the presence of two adjacent nitrogen atoms in the 2-aminopyrimidine or 2-aminopyridine moieties. The only 2-aminopyrimidine derivative which shows chelating ability also towards Zn^{2+} ion is **20**, which contains a catechol group.

Moreover, antioxidant activity assays were carried out on compounds **18**, **19**, **20** and **30**, since they are the most potent ChEs inhibitors among phenolic derivatives. The catechol **20** is the most efficient antioxidant, even better than ascorbic acid, both for the high reaction rate with DPPH and for its EC_{50} value. Compounds **18** and **30**, having the 3-methoxy-4-hydroxyphenyl ring, show antioxidant capacity lower than **20** and comparable to each other, while compound **19**, having the 3-hydroxyphenyl ring, has not significant antioxidant capacity.

Unfortunately, the tested compounds show low percentages of inhibition both towards $\text{A}\beta_{42}$ and Tau aggregation, proving to have weak anti-aggregating activity in *E. coli*. However, the low anti-amyloid activity reported could also be due to an unusually low ability of the compounds to cross the bacterial wall. Although it is unusual, this effect has been observed recently and should not be ruled out.³⁹

In conclusion, this research has allowed to identify interesting lead compounds for the development of new multi-functional molecules useful for AD, by virtue of their inhibitory activity towards ChEs, as well as for chelating and antioxidant abilities, low toxicity and good predicted ADME parameters.

Experimental section

Chemistry: General. All reagents and solvents were of analytical grade and were purchased from Sigma-Aldrich (Milano, Italy) or from Fluorochem (Hadfield, UK). Dichloromethane

was dried storing it over activated 4Å molecular sieves (10% m/v). Triethylamine was freshly purified by distillation over potassium hydroxide. Column chromatographies were performed on silica gel (Merck; 63–200 µm particle size). ¹H-NMR and ¹³C-NMR spectra were acquired at 25°C, unless otherwise specified, on Bruker AVANCE-400 spectrometer at 9.4 Tesla operating at 400 MHz (¹H-NMR) and 100 MHz (¹³C-NMR); chemical shift values (δ) are given in ppm relatively to TMS as internal reference; coupling constants are given in Hz. The following abbreviations were used: s = singlet, d = doublet, t = triplet, q = quartet, dd = double doublet, ddd = double double doublet, bs = broad singlet, m = multiplet. Mass spectra were recorded on a ThermoFinnigan LCQ Classic LC/MS/MS ion trap equipped with an ESI source and a syringe pump; samples (10⁻⁴-10⁻⁵ M in MeOH/H₂O 80:20) were infused in the electrospray system at a flow rate of 5-10 µL min⁻¹; when necessary, 50 µL of 10⁻² M HCOOH or 10⁻² M NH₃ were added to the sample solutions, in order to promote the analyte ionization; the ESI-MS data are given as m/z, with mass expressed in amu. Melting points were determined on FALC Mod. 360 D apparatus and are uncorrected. Infrared spectra were recorded on a Perkin Elmer Spectrum One FT-IR spectrometer equipped with an ATR system. The purity of the compounds was determined by elemental analyses obtained by a PE 2400 (Perkin-Elmer) analyzer and the analytical results were within ± 0.4 % of the theoretical values for all compounds.

General Experimental Procedures

General Procedure A (GP-A) for the Synthesis of Pyrimidine Intermediates 1-2

To a solution of *N*-Boc-1,5-diaminopentane (1 eq) or *N*-Boc-1,6-diaminohexane (1 eq) in 20 mL of MeOH, TEA (1 eq) and 2-chloropyrimidine (1 eq) were added. The reaction mixture was stirred at reflux for 20 hours. Then it was cooled to room temperature and the solvent was removed under reduced pressure. The residue was diluted with a saturated aqueous solution of Na₂CO₃ (25 mL) and extracted with CH₂Cl₂ (3 × 25 mL). The combined organic layer was

dried over Na₂SO₄, filtered and the solvent was evaporated under reduced pressure. The crude material was purified by column chromatography on silica gel (CH₂Cl₂/MeOH 9.5:0.5). For each compound R_f; yield (%); ¹H NMR; ESI-MS and elemental analysis are reported.

General Procedures (GP-B) for the Synthesis of *N*¹-(pyrimidin-2-yl)pentane-1,5-diamine (3), *N*¹-(pyrimidin-2-yl)hexane-1,6-diamine (4), *N*¹-(pyridin-2-yl)pentane-1,5-diamine (7) and *N*¹-(pyridin-2-yl)hexane-1,6-diamine (8)

Procedure 1: Intermediates **1**, **2**, **5** or **6** (1 eq), respectively used for synthesis of compounds **3**, **4**, **7** and **8**, were dissolved in 20 mL of dry CH₂Cl₂ and to the solution TFA (20 eq) was added. The mixture was stirred at room temperature for 3.5 hours and then the solvent and the excess of TFA were removed under reduce pressure to give trifluoroacetic salts of compounds **3**, **4**, **7** or **8**, as yellow oils, which were used for the subsequent reactions without further purification.

Procedure 2: To a solution of intermediate **2** or **6** (1 eq) in 20 mL of dry CH₂Cl₂ TFA (20 eq) was added. The mixture was stirred at room temperature for 3.5 hours and then it was extracted twice with 5N NaOH solution (2 x 20 mL), once with H₂O (20 mL). The organic layer was dried over Na₂SO₄, filtered and the solvent was removed under vacuum to give compounds **4** (77% yield) or **8** (88% yield) as yellow oils, which were used for the subsequent reactions without further purification.

Procedure 3: To a solution of 1,6-diaminohexane (1.516 g, 13.05 mmol) in 10 mL of MeOH TEA (605 μL, d=0.726 g/mL, 4.35 mmol) and 2-chloropyrimidine (0.498 g, 4.35 mmol) were added. The reaction mixture was stirred at reflux for 20 hours. Then it was cooled to room temperature and the solvent was removed under reduced pressure. The residue was diluted with a saturated aqueous solution of Na₂CO₃ (15 mL) and extracted with CH₂Cl₂ (3 × 20 mL). The combined organic layer was dried over Na₂SO₄, filtered and concentrated under reduced pressure. The crude material was purified by column chromatography on silica gel

(MeOH/CH₂Cl₂/TEA 8:2:0.2, R_f = 0.17) and subsequently the product was filtered with warm acetonitrile to afford compound **4**.

General procedure C (GP-C) for the synthesis of pyridine intermediates 5-6

An oven-dried Schlenk flask equipped with a Teflon valve was charged with *N*-Boc-1,5-diaminopentane or *N*-Boc-1,6-diaminohexane (1.5 eq), CuI (0.05 eq), Cs₂CO₃ (2 eq) and with a magnetic stir bar. The flask was closed, evacuated and backfilled with N₂ for at least 10 minutes. Under a counter flow of N₂, DMF (0.5 mL), 2-iodopyridine (1 eq) and finally 2-isobutyrylcyclohexanone (0.2 eq) were added by syringe. The mixture was allowed to stir under N₂ at 40°C for 21 hours. After this period the mixture was diluted with ethyl acetate, transferred to a centrifuge tube and centrifuged to separate the inorganic salts. The solvent was removed under reduced pressure. The crude residue was purified by column chromatography on silica gel (CH₂Cl₂/MeOH 9.5:0.5). For each compound R_f, yield (%); ¹H NMR; ESI-MS and elemental analysis are reported.

General procedures D (GP-D) for the synthesis of pyrimidine and pyridine diamine derivatives 9-33.

Procedure 1: Intermediates **3**, **4**, **7** or **8** (1 eq), obtained following procedure 1 of GP-B described above, were dissolved in 20 mL of dry CH₂Cl₂ and to the solution the opportune aldehyde (1 eq) and dry K₂CO₃ (20 eq) were added. The mixture was stirred at room temperature for 12 hours and then filtered. The solvent was removed under reduced pressure and the residue was dissolved in 30 mL of MeOH and treated with NaBH₄ (3 eq) at room temperature for 2 hours. Then 5 mL of H₂O were added; after 5 minutes under stirring MeOH was evaporated under reduced pressure, H₂O (20 mL) was added and the mixture was extracted with CH₂Cl₂ (3 x 20 mL). The organic layer was dried over Na₂SO₄ and the solvent was removed under vacuum. The obtained residue was purified by column chromatography on

silica gel. For each compound chromatography system; R_f ; yield (%); ^1H NMR; ^{13}C -NMR; ESI-MS; IR; melting point ($^\circ\text{C}$) and elemental analysis are reported.

Procedure 2: Intermediate **4** (1 eq), obtained following procedure 2 of GP-B described above, was dissolved in 20 mL of dry CH_2Cl_2 and to the solution the opportune aldehyde (1 eq) and molecular sieves (4 Å) were added. The mixture was stirred at room temperature for 12 hours and then filtered. The solvent was removed under reduced pressure and the residue was dissolved in 30 mL of MeOH and treated with NaBH_4 (3 eq) at room temperature for 2 hours. Then 5 mL of H_2O were added; after 5 minutes under stirring MeOH was evaporated under reduced pressure, H_2O (20 mL) was added and the mixture was extracted with CH_2Cl_2 (3 x 20 mL). The organic layer was dried over Na_2SO_4 and the solvent was removed under vacuum. The obtained residue was purified by column chromatography on silica gel. For each compound chromatography system; R_f ; yield (%); ^1H NMR; ^{13}C -NMR; ESI-MS; IR; melting point ($^\circ\text{C}$) and elemental analysis are reported.

Procedure 3: Intermediates **4** or **8** (1 eq), obtained following respectively procedure 3 or 2 of GP-B described above, were dissolved in 20 mL of dry CH_2Cl_2 and to the solution the opportune aldehyde (1 eq) and molecular sieves (4 Å) were added. The mixture was stirred at room temperature for 12 hours and then filtered. The solvent was removed under reduced pressure and the residue was dissolved in 30 mL of MeOH and treated with NaBH_4 (3 eq) at room temperature for 2 hours. Then 5 mL of 1M HCl were added; after 5 minutes under stirring the solvent was evaporated under reduced pressure, the residue was diluted with 20 mL of saturated aqueous solution of NaHCO_3 and extracted with CH_2Cl_2 (3 x 20 mL). The organic layer was dried over Na_2SO_4 and the solvent was removed under vacuum. The obtained residue was purified by column chromatography on silica gel and/or by crystallization. For each compound chromatography system (and/or crystallization solvent); R_f ; yield (%); ^1H NMR; ^{13}C -NMR; ESI-MS; IR; melting point ($^\circ\text{C}$) and elemental analysis are reported.

Tert-butyl {5-[(pyrimidin-2-yl)amino]pentyl}carbamate (1)

Compound **1** was prepared using *N*-Boc-1,5-diaminopentane (0.773 g, 3.82 mmol), TEA (531 μ L, $d=0.726$ g/mL, 3.82 mmol) and 2-chloropyrimidine (0.438 g, 3.82 mmol), following GP-A. R_f ($\text{CH}_2\text{Cl}_2/\text{MeOH}$ 9.5:0.5) = 0.34. White solid, 0.539 g, 50% yield. $^1\text{H-NMR}$ (400 MHz) (CD_3CN) δ (ppm): 8.22 (d, 2H, $J = 4.76$ Hz, pyrimidine); 6.51 (t, 1H, $J = 4.80$ Hz, pyrimidine); 5.68 (bs, 1H, pyrimidine-NH-); 5.26 (bs, 1H, Boc-NH-); 3.32 (q, 2H, $J = 6.88$ Hz, pyrimidine-NH-CH₂-); 3.00 (q, 2H, $J = 6.60$ Hz, Boc-NH-CH₂-); 1.60-1.53 (m, 2H, pyrimidine-NH-CH₂-CH₂-); 1.49-1.30 (m, 13H, pyrimidine-NH-CH₂-CH₂-CH₂-CH₂-CH₂-NH-COO-C(CH₃)₃). ESI-MS (m/z): $[\text{M}+\text{H}]^+ = 280.79$. Anal. ($\text{C}_{14}\text{H}_{24}\text{N}_4$) C, H, N Calcd: C 59.98 %, H 8.63 %, N 19.98 %; Found: C 59.89 %, H 8.59 %, N 19.90 %.

Tert-butyl {6-[(pyrimidin-2-yl)amino]hexyl}carbamate (2)

Compound **2** was prepared using *N*-Boc-1,6-diaminohexane (0.437 g, 2.02 mmol), TEA (281 μ L, $d=0.726$ g/mL, 2.02 mmol) and 2-chloropyrimidine (0.231 g, 2.02 mmol), following GP-A. R_f ($\text{CH}_2\text{Cl}_2/\text{MeOH}$ 9.5:0.5) = 0.5. White solid, 0.358 g, 60% yield. $^1\text{H-NMR}$ (400 MHz) (CD_3CN) δ (ppm): 8.22 (d, 2H, $J = 4.40$ Hz, pyrimidine); 6.51 (t, 1H, $J = 4.20$ Hz, pyrimidine); 5.69 (bs, 1H, pyrimidine-NH-); 5.24 (bs, 1H, Boc-NH-); 3.32 (q, 2H, $J = 6.48$ Hz, pyrimidine-NH-CH₂-); 3.00 (q, 2H, $J = 6.16$ Hz, Boc-NH-CH₂-); 1.59-1.52 (m, 2H, pyrimidine-NH-CH₂-CH₂-); 1.46-1.23 (m, 15H, pyrimidine-NH-CH₂-CH₂-CH₂-CH₂-CH₂-CH₂-CH₂-NH-COO-C(CH₃)₃). ESI-MS (m/z): $[\text{M}+\text{H}]^+ = 294.73$. Anal. ($\text{C}_{15}\text{H}_{26}\text{N}_4$) C, H, N Calcd: C 61.20 %, H 8.90 %, N 19.03 %; Found: C 60.97 %, H 8.86 %, N 18.96 %.

***N*¹-(pyrimidin-2-yl)pentane-1,5-diamine (3)**

Compound **3** was prepared following procedure 1 of GP-B as trifluoroacetic salt and used for the subsequent reactions without purification.

***N*¹-(pyrimidin-2-yl)hexane-1,6-diamine (4)**

Compound **4** was prepared following procedure 1 of GP-B as trifluoroacetic salt (used for the subsequent reactions without purification) or following procedure 2 or 3 of GP-B as free amine. Yellow wax, 0.590 g, 70% yield. ¹H-NMR (400 MHz) (MeOD) δ (ppm): 8.24 (d, 2H, $J = 4.84$ Hz, pyrimidine); 6.57 (t, 1H, $J = 4.88$ Hz, pyrimidine); 3.35 (t, 2H, $J = 7.08$ Hz, pyrimidine-NH-CH₂-); 2.71 (t, 2H, $J = 7.20$ Hz; -CH₂-NH₂); 1.66-1.40 (m, 8H, pyrimidine-NH-CH₂-CH₂-CH₂-CH₂-NH₂). ESI-MS (m/z): $[M+H]^+ = 194.70$. Anal. (C₁₀H₁₈N₄) C, H, N Calcd: C 61.82 %, H 9.34 %, N 28.84 %; Found: C 61.58 %, H 9.30 %, N 28.73 %.

***Tert*-butyl {5-[(pyridin-2-yl)amino]pentyl}carbamate (5)**

Compound **5** was prepared using *N*-Boc-1,5-diaminopentane (0.303 g, 1.5 mmol), CuI (0.095 g, 0.05 mmol), Cs₂CO₃ (0.652 g, 2 mmol), DMF (0.5 mL), 2-iodopyridine (107 μ L, $d=1.928$ g/mL, 1 mmol) and 2-isobutyrylcyclohexanone (33 μ L, $d=1.008$ g/mL, 0.2 mmol) following GP-C. R_f (CH₂Cl₂/MeOH 9.5:0.5) = 0.38. Yellowish solid, 0.279 g, 100% yield. ¹H-NMR (400 MHz) (CD₃CN) δ (ppm): 7.97 (d, 1H, $J = 4.08$ Hz, pyridine); 7.39-7.35 (m, 1H, pyridine); 6.50-6.47 (m, 1H, pyridine); 6.41 (d, 1H, $J = 8.44$ Hz, pyridine); 5.26 (bs, 1H, Boc-NH-); 5.09 (bs, 1H, pyridine-NH-); 3.23 (q, 2H, $J = 6.92$ Hz, pyridine-NH-CH₂-); 3.01 (q, 2H, $J = 6.60$ Hz, Boc-NH-CH₂-); 1.60-1.53 (m, 2H, pyridine-NH-CH₂-CH₂-); 1.50-1.31 (m, 13H, pyridine-NH-CH₂-CH₂-CH₂-CH₂-CH₂-NH-COO-C(CH₃)₃). ESI-MS (m/z): $[M+H]^+ = 280.00$. Anal. (C₁₅H₂₅N₃) C, H, N Calcd: C 64.49 %, H 9.02 %, N 15.04 %; Found: C 64.25 %, H 8.98 %, N 14.98 %.

***Tert*-butyl {6-[(pyridin-2-yl)amino]hexyl}carbamate (6)**

Compound **6** was prepared using *N*-Boc-1,6-diaminohexane (0.811 g, 3.75 mmol), CuI (0.024 g, 0.125 mmol), Cs₂CO₃ (1.63 g, 5 mmol), DMF (1.25 mL), 2-iodopyridine (267 μ L, $d=1.928$ g/mL, 2.5 mmol) and 2-isobutyrylcyclohexanone (83 μ L, $d=1.008$ g/mL, 0.5 mmol) following GP-C. R_f (CH₂Cl₂/MeOH 9.5:0.5) = 0.38. Yellowish solid, 0.734 g, 100% yield. ¹H-NMR (400 MHz) (CD₃CN) δ (ppm): 7.97 (dd, 1H, $J_1 = 5.00$ Hz, $J_2 = 1.12$ Hz, pyridine); 7.39-

7.35 (m, 1H, pyridine); 6.50-6.47 (m, 1H, pyridine); 6.40 (d, 1H, $J = 8.40$ Hz, pyridine); 5.25 (bs, 1H, Boc-NH-); 5.09 (bs, 1H, pyridine-NH-); 3.23 (q, 2H, $J = 6.96$ Hz, pyridine-NH-CH₂-); 3.00 (q, 2H, $J = 6.64$ Hz, Boc-NH-CH₂-); 1.59-1.52 (m, 2H, pyridine-NH-CH₂-CH₂-); 1.46-1.27 (m, 15H, pyridine-NH-CH₂-CH₂-CH₂-CH₂-CH₂-CH₂-CH₂-NH-COO-C(CH₃)₃). ESI-MS (m/z): $[M+H]^+ = 293.87$. Anal. (C₁₆H₂₇N₃) C, H, N Calcd: C 65.50 %, H 9.28 %, N 14.32 %; Found: C 65.24 %, H 9.24 %, N 14.26 %.

***N*¹-(pyridin-2-yl)pentane-1,5-diamine (7)**

Compound **7** was prepared following procedure 1 of GP-B as trifluoroacetic salt and used for the subsequent reactions without purification.

***N*¹-(pyridin-2-yl)hexane-1,6-diamine (8)**

Compound **8** was prepared following procedure 1 of GP-B as trifluoroacetic salt or following procedure 2 of GP-B as free amine and used for the subsequent reactions without purification.

***N*¹-benzyl-*N*⁵-(pyrimidin-2-yl)pentane-1,5-diamine (9)**

Compound **9** was prepared using *N*¹-(pyrimidin-2-yl)pentane-1,5-diamine (**3**) (0.108 g, 0.60 mmol), benzaldehyde (61 μ L, $d = 1.045$ g/mL, 0.60 mmol), K₂CO₃ (1.659 g, 12.0 mmol), NaBH₄ (0.068 g, 1.8 mmol), following the procedure 1 of GP-D described above. Column chromatography: silica gel, CH₂Cl₂/MeOH 1:1, $R_f = 0.4$. White solid, 0.093 g, 57% yield. ¹H-NMR (400 MHz) (CD₃CN) δ (ppm): 8.22 (d, 2H, $J = 4.72$ Hz, pyrimidine); 7.31-7.20 (m, 5H, aromatic); 6.50 (t, 1H, $J = 4.76$ Hz, pyrimidine); 5.69 (bs, 1H, pyrimidine-NH-); 3.71 (s, 2H, Ar-CH₂-NH-); 3.32 (q, 2H, $J = 6.88$ Hz, pyrimidine-NH-CH₂-); 2.54 (t, 2H, $J = 6.92$ Hz, Ar-CH₂-NH-CH₂-); 1.59-1.45 (m, 4H, -NH-CH₂-CH₂-CH₂-CH₂-NH-); 1.41-1.34 (m, 2H, -NH-CH₂-CH₂-CH₂-CH₂-NH-). ¹³C-NMR (100 MHz) (CD₃CN) δ (ppm): 163.7; 158.9; 142.4; 129.1; 128.9; 127.5; 111.0; 54.3; 49.9; 41.8; 30.5; 30.1; 25.4. ESI-MS (m/z): $[M+H]^+ = 270.87$. I.R. (cm⁻¹): ν_{N-H} : 3255; finger print: 1124, 1100, 1074, 1027. m.p. = 58.0-59.8 °C.

Anal. (C₁₆H₂₂N₄) C, H, N Calcd: C 71.08 %, H 8.20 %, N 20.72 %; Found: C 70.98 %, H 8.23 %, N 20.79 %.

***N*¹-(4-bromobenzyl)-*N*⁵-(pyrimidin-2-yl)pentane-1,5-diamine (10)**

Compound **10** was prepared using *N*¹-(pyrimidin-2-yl)pentane-1,5-diamine (**3**) (0.097 g, 0.54 mmol), 4-bromobenzaldehyde (0.100 g, 0.54 mmol), K₂CO₃ (1.493 g, 10.8 mmol), NaBH₄ (0.061 g, 1.62 mmol), following the procedure 1 of GP-D described above. Column chromatography: silica gel, CH₂Cl₂/MeOH 1:1, R_f = 0.5. White solid, 0.093 g, 50% yield. ¹H-NMR (400 MHz) (CD₃CN) δ (ppm): 8.22 (d, 2H, *J* = 4.76 Hz, pyrimidine); 7.45 (d, 2H, *J* = 8.40 Hz, aromatic); 7.25 (d, 2H, *J* = 8.44 Hz, aromatic); 6.51 (t, 1H, *J* = 4.80 Hz, pyrimidine); 5.68 (bs, 1H, pyrimidine-NH-); 3.68 (s, 2H, Ar-CH₂-NH-); 3.32 (q, 2H, *J* = 6.92 Hz, pyrimidine-NH-CH₂-); 2.52 (t, 2H, *J* = 6.84 Hz, Ar-CH₂-NH-CH₂-); 1.59-1.44 (m, 4H, -NH-CH₂-CH₂-CH₂-CH₂-CH₂-NH-); 1.41-1.33 (m, 2H, -NH-CH₂-CH₂-CH₂-CH₂-CH₂-NH-). ¹³C-NMR (100 MHz) (MeOD) δ (ppm): 163.5; 159.2; 140.0; 132.5; 131.5; 121.8; 111.0; 53.7; 50.0; 42.0; 30.3; 30.1; 25.7. ESI-MS (*m/z*): [M+H]⁺ = 348.80 (95); 350.80 (100). I.R. (cm⁻¹): ν_{N-H}: 3235; finger print: 1265, 1129, 1066, 1007. m.p. = 75.2-77.0 °C. Anal. (C₁₆H₂₁BrN₄) C, H, N Calcd: C 55.02 %, H 6.06 %, N 16.04 %; Found: C 54.95 %, H 6.08 %, N 16.09 %.

***N*¹-(2-methoxybenzyl)-*N*⁵-(pyrimidin-2-yl)pentane-1,5-diamine (11)**

Compound **11** was prepared using *N*¹-(pyrimidin-2-yl)pentane-1,5-diamine (**3**) (0.108 g, 0.60 mmol), 2-methoxybenzaldehyde (0.082 g, 0.60 mmol), K₂CO₃ (1.659 g, 12.0 mmol), NaBH₄ (0.068 g, 1.8 mmol), following the procedure 1 of GP-D described above. Column chromatography: silica gel, CH₂Cl₂/MeOH 1:1, R_f = 0.3. Pale yellow solid, 0.091 g, 50% yield. ¹H-NMR (400 MHz) (CD₃CN) δ (ppm): 8.22 (d, 2H, *J* = 4.76 Hz, pyrimidine); 7.26-7.20 (m, 2H, aromatic); 6.94-6.87 (m, 2H, aromatic); 6.50 (t, 1H, *J* = 4.80 Hz, pyrimidine); 5.68 (bs, 1H, pyrimidine-NH-); 3.80 (s, 3H, -O-CH₃); 3.68 (s, 2H, Ar-CH₂-NH-); 3.32 (q, 2H, *J* = 6.92 Hz, pyrimidine-NH-CH₂-); 2.53 (t, 2H, *J* = 6.92 Hz, Ar-CH₂-NH-CH₂-); 1.59-1.45 (m, 4H, -

NH-CH₂-CH₂-CH₂-CH₂-CH₂-NH-); 1.40-1.33 (m, 2H, -NH-CH₂-CH₂-CH₂-CH₂-CH₂-NH-). ¹³C-NMR (100 MHz) (MeOD) δ (ppm): 163.5; 159.23; 159.19; 131.2; 129.8; 128.2; 121.5; 111.5; 111.0; 55.8; 49.8; 49.6; 42.0; 30.3; 30.0; 25.7. ESI-MS (*m/z*): [M+H]⁺ = 301.02. I.R. (cm⁻¹): ν_{N-H}: 3247; finger print: 1293, 1266, 1235, 1100, 1050, 1023, 932. m.p. = 44.8-46.8 °C. Anal. (C₁₇H₂₄N₄O) C, H, N Calcd: C 67.97 %, H 8.05 %, N 18.65 %; Found: C 67.98 %, H 8.07 %, N 18.60 %.

***N*¹-((2,6-dichloropyridin-4-yl)methyl)-*N*⁵-(pyrimidin-2-yl)pentane-1,5-diamine (12)**

Compound **12** was prepared using *N*¹-(pyrimidin-2-yl)pentane-1,5-diamine (**3**) (0.090 g, 0.50 mmol), 2,6-dichloropyridine-4-carbaldehyde (0.088 g, 0.50 mmol), K₂CO₃ (1.382 g, 10.0 mmol), NaBH₄ (0.057 g, 1.5 mmol), following the procedure 1 of GP-D described above. Column chromatography: silica gel, AcOEt/MeOH 1:1, R_f = 0.5. Pale yellow solid, 0.094 g, 55% yield. ¹H-NMR (400 MHz) (CD₃CN) δ (ppm): 8.22 (d, 2H, *J* = 4.72 Hz, pyrimidine); 7.36 (s, 2H, pyridine); 6.50 (t, 1H, *J* = 4.76 Hz, pyrimidine); 5.67 (bs, 1H, pyrimidine-NH-); 3.75 (s, 2H, pyridine-CH₂-NH-); 3.32 (q, 2H, *J* = 6.88 Hz, pyrimidine-NH-CH₂-); 2.52 (t, 2H, *J* = 6.84 Hz, pyridine-CH₂-NH-CH₂-); 1.60-1.45 (m, 4H, -NH-CH₂-CH₂-CH₂-CH₂-NH-); 1.42-1.34 (m, 2H -NH-CH₂-CH₂-CH₂-CH₂-NH-). ¹³C-NMR (100 MHz) (MeOD) δ (ppm): 163.5; 159.2; 157.7; 151.4; 123.6; 111.0; 52.4; 50.1; 42.1; 30.5; 30.6; 25.9. ESI-MS (*m/z*): [M+H]⁺ = 340.09 (100); 342.08 (65); 344.06 (10). Anal. (C₁₅H₁₉Cl₂N₅) C, H, N Calcd: C 52.95 %, H 5.63 %, N 20.58 %; Found: C 52.91 %, H 5.62 %, N 20.61 %.

***N*¹-benzyl-*N*⁶-(pyrimidin-2-yl)hexane-1,6-diamine (13)**

Compound **13** was prepared using *N*¹-(pyrimidin-2-yl)hexane-1,6-diamine (**4**) (0.103 g, 0.53 mmol), benzaldehyde (54 μL, d=1.045 g/mL, 0.53 mmol), K₂CO₃ (1.465 g, 10.6 mmol), NaBH₄ (0.060 g, 1.59 mmol), following the procedure 1 of GP-D described above. Column chromatography: silica gel, CH₂Cl₂/MeOH 7:3, R_f = 0.42. White solid, 0.066 g, 43% yield. ¹H-NMR (400 MHz) (CD₃CN) δ (ppm): 8.22 (d, 2H, *J* = 4.76 Hz, pyrimidine); 7.33-7.20 (m, 5H,

aromatic); 6.50 (t, 1H, $J = 4.80$ Hz, pyrimidine); 5.74 (bs, 1H, pyrimidine-NH-); 3.71 (s, 2H, Ar-CH₂-NH-); 3.31 (q, 2H, $J = 6.84$ Hz, pyrimidine-NH-CH₂-); 2.53 (t, 2H, $J = 7.04$ Hz, Ar-CH₂-NH-CH₂-); 1.59-1.52 (m, 2H, -NH-CH₂-CH₂-); 1.49-1.41 (m, 2H, -NH-CH₂-CH₂-); 1.38-1.27 (m, 4H -NH-CH₂-CH₂-CH₂-CH₂-CH₂-NH-). ¹³C-NMR (100 MHz) (CD₃CN) δ (ppm): 163.7; 158.9; 142.2; 129.1; 129.0; 127.5; 111.0; 54.3; 49.9; 41.8; 30.6; 30.2; 27.8; 27.5. ESI-MS (m/z): [M+H]⁺ = 285.13. I.R. (cm⁻¹): ν_{N-H} : 3301, 3267; finger print: 1323, 1258, 1129, 1027, 984, 975. m.p. = 51.8-54.4 °C. Anal. (C₁₇H₂₄N₄) C, H, N Calcd: C 71.79 %, H 8.51 %, N 19.70 %; Found: C 71.89 %, H 8.47 %, N 19.64 %.

***N*¹-(4-bromobenzyl)-*N*⁶-(pyrimidin-2-yl)hexane-1,6-diamine (14)**

Compound **14** was prepared using *N*¹-(pyrimidin-2-yl)hexane-1,6-diamine (**4**) (0.136 g, 0.70 mmol), 4-bromobenzaldehyde (0.130 g, 0.70 mmol), K₂CO₃ (1.935 g, 14.0 mmol), NaBH₄ (0.079 g, 2.1 mmol), following the procedure 1 of GP-D described above. Column chromatography: silica gel, CH₂Cl₂/MeOH 1:1, R_f = 0.4. White solid, 0.152 g, 60% yield. ¹H-NMR (400 MHz) (CD₃CN) δ (ppm): 8.21 (d, 2H, $J = 4.72$ Hz, pyrimidine); 7.45 (d, 2H, $J = 8.32$ Hz, aromatic); 7.24 (d, 2H, $J = 8.28$ Hz, aromatic); 6.50 (t, 1H, $J = 4.76$ Hz, pyrimidine); 5.77 (bs, 1H, pyrimidine-NH-); 3.67 (s, 2H, Ar-CH₂-NH-); 3.31 (q, 2H, $J = 6.68$ Hz, pyrimidine-NH-CH₂-); 2.50 (t, 2H, $J = 6.92$ Hz, Ar-CH₂-NH-CH₂-); 1.58-1.51 (m, 2H, -NH-CH₂-CH₂-); 1.47-1.41 (m, 2H, -NH-CH₂-CH₂-); 1.37-1.26 (m, 4H -NH-CH₂-CH₂-CH₂-CH₂-CH₂-NH-). ¹³C-NMR (100 MHz) (CD₃CN) δ (ppm): 163.7; 158.9; 141.8; 132.0; 130.9; 120.6; 111.0; 53.5; 49.8; 41.8; 30.7; 30.2; 27.7; 27.5. ESI-MS (m/z): [M+H]⁺ = 363.07 (95); 365.00 (100). I.R. (cm⁻¹): ν_{N-H} : 3267; finger print: 1255, 1132, 1068, 1010. m.p. = 43-46 °C. Anal. (C₁₇H₂₃BrN₄) C, H, N Calcd: C 56.20 %, H 6.38 %, N 15.42 %; Found: C 56.21 %, H 6.39 %, N 15.45 %.

***N*¹-(4-chlorobenzyl)-*N*⁶-(pyrimidin-2-yl)hexane-1,6-diamine (15)**

Compound **15** was prepared using *N*¹-(pyrimidin-2-yl)hexane-1,6-diamine (**4**) (0.107 g, 0.55 mmol), 4-chlorobenzaldehyde (0.077 g, 0.55 mmol), K₂CO₃ (1.520 g, 11.0 mmol), NaBH₄ (0.062 g, 1.65 mmol), following the procedure 1 of GP-D described above. Column chromatography: silica gel, CH₂Cl₂/MeOH 7:3, R_f = 0.53. White solid, 0.085 g, 50% yield. ¹H-NMR (400 MHz) (CD₃CN) δ (ppm): 8.22 (d, 2H, *J* = 4.76 Hz, pyrimidine); 7.31 (s, 4H, aromatic); 6.50 (t, 1H, *J* = 4.76 Hz, pyrimidine); 5.71 (bs, 1H, pyrimidine-NH-); 3.69 (s, 2H, Ar-CH₂-NH-); 3.31 (q, 2H, *J* = 6.84 Hz, pyrimidine-NH-CH₂-); 2.51 (t, 2H, *J* = 6.92 Hz, Ar-CH₂-NH-CH₂-); 1.58-1.51 (m, 2H, -NH-CH₂-CH₂-); 1.48-1.41 (m, 2H, -NH-CH₂-CH₂-); 1.38-1.27 (m, 4H -NH-CH₂-CH₂-CH₂-CH₂-CH₂-CH₂-NH-). ¹³C-NMR (100 MHz) (CD₃CN) δ (ppm): 163.7; 158.9; 141.3; 132.5; 130.6; 129.0; 111.0; 53.5; 49.8; 41.8; 30.6; 30.2; 27.7; 27.5. ESI-MS (*m/z*): [M+H]⁺ = 318.87 (100); 320.87 (30). I.R. (cm⁻¹): ν_{N-H}: 3264; finger print: 1256, 1132, 1123, 1088, 1012, 987. m.p. = 53-56 °C. Anal. (C₁₇H₂₃ClN₄) C, H, N Calcd: C 64.04 %, H 7.27 %, N 17.57 %; Found: C 64.08 %, H 7.26 %, N 17.52 %.

*N*¹-(2-methoxybenzyl)-*N*⁶-(pyrimidin-2-yl)hexane-1,6-diamine (**16**)

Compound **16** was prepared using *N*¹-(pyrimidin-2-yl)hexane-1,6-diamine (**4**) (0.185 g, 0.95 mmol), 2-methoxybenzaldehyde (0.129 g, 0.95 mmol), K₂CO₃ (2.626 g, 19.0 mmol), NaBH₄ (0.108 g, 2.85 mmol), following the procedure 1 of GP-D described above. Column chromatography: silica gel, CH₂Cl₂/MeOH 1:1, R_f = 0.23. Pale yellow oil, 0.184 g, 62% yield. ¹H-NMR (400 MHz) (CD₃CN) δ (ppm): 8.22 (d, 2H, *J* = 4.76 Hz, pyrimidine); 7.28-7.21 (m, 2H, aromatic); 6.94-6.88 (m, 2H, aromatic); 6.50 (t, 1H, *J* = 4.76 Hz, pyrimidine); 5.70 (bs, 1H, pyrimidine-NH-); 3.81 (s, 3H, -O-CH₃); 3.71 (s, 2H, Ar-CH₂-NH-); 3.32 (q, 2H, *J* = 6.76 Hz, pyrimidine-NH-CH₂-); 2.54 (t, 2H, *J* = 6.96 Hz, Ar-CH₂-NH-CH₂-); 1.58-1.44 (m, 4H, -NH-CH₂-CH₂-CH₂-CH₂-CH₂-CH₂-NH-); 1.40-1.28 (m, 4H, -NH-CH₂-CH₂-CH₂-CH₂-CH₂-). ¹³C-NMR (100 MHz) (CD₃CN) δ (ppm): 163.9; 159.0; 158.8; 130.5; 129.6; 129.1; 121.3; 111.6; 111.1; 56.1; 49.9; 49.3; 42.0; 30.6; 30.3; 27.9; 27.6. ESI-MS (*m/z*): [M+H]⁺ =

315.13. I.R. (cm^{-1}): $\nu_{\text{N-H}}$: 3265; finger print: 1240, 1104, 1031. Anal. ($\text{C}_{18}\text{H}_{26}\text{N}_4\text{O}$) C, H, N Calcd: C 68.76 %, H 8.33 %, N 17.82 %; Found: C 68.70 %, H 8.30 %, N 17.78 %.

***N*¹-(pyrimidin-2-yl)-*N*⁶-(3,4,5-trimethoxybenzyl)hexane-1,6-diamine (17)**

Compound **17** was prepared using *N*¹-(pyrimidin-2-yl)hexane-1,6-diamine (**4**) (0.101 g, 0.52 mmol), 3,4,5-trimethoxybenzaldehyde (0.102 g, 0.52 mmol), NaBH_4 (0.059 g, 1.56 mmol), following the procedure 3 of GP-D described above. Column chromatography: silica gel, AcOEt/MeOH 1:1, R_f = 0.23. Yellow oil, 0.138 g, 71% yield. ¹H-NMR (400 MHz) (Acetone-*d*₆) δ (ppm): 8.22 (d, 2H, J = 4.68 Hz, pyrimidine); 6.67 (s, 2H, aromatic); 6.50 (t, 1H, J = 4.76 Hz, pyrimidine); 6.26 (bs, 1H, pyrimidine-NH-); 3.79 (s, 6H, Ar-(OCH₃)₂); 3.69 (s, 3H, Ar-OCH₃); 3.68 (s, 2H, Ar-CH₂-NH-); 3.40-3.35 (m, 2H, pyrimidine-NH-CH₂-); 2.57 (t, 2H, J = 6.84 Hz, Ar-CH₂-NH-CH₂-); 1.64-1.57 (m, 2H, -NH-CH₂-CH₂-); 1.54-1.47 (m, 2H, -NH-CH₂-CH₂-); 1.43-1.37 (m, 4H, -NH-CH₂-CH₂-CH₂-CH₂-CH₂-NH-). ¹³C-NMR (100 MHz) (MeOD) δ (ppm): 163.5; 159.2; 154.5; 138.2; 136.3; 111.0; 106.9; 61.1; 56.6; 54.5; 49.8; 42.1; 30.4; 30.1; 28.2; 27.9. ESI-MS (m/z): $[\text{M}+\text{H}]^+$ = 374.67. I.R. (cm^{-1}): $\nu_{\text{N-H}}$: 3276; finger print: 1233, 1121, 1007. Anal. ($\text{C}_{20}\text{H}_{30}\text{N}_4\text{O}_3$) C, H, N Calcd: C 64.15 %, H 8.07 %, N 14.96 %; Found: C 64.09 %, H 8.09 %, N 15.01 %.

2-methoxy-4-(((6-(pyrimidin-2-ylamino)hexyl)amino)methyl)phenol (18)

Compound **18** was prepared using *N*¹-(pyrimidin-2-yl)hexane-1,6-diamine (**4**) (0.117 g, 0.60 mmol), 4-hydroxy-3-methoxybenzaldehyde (0.091 g, 0.60 mmol), NaBH_4 (0.068 g, 1.80 mmol), following the procedure 3 of GP-D described above. Column chromatography: silica gel, AcOEt/MeOH/TEA 5:5:0.1, R_f = 0.37. White solid, 0.135 g, 68% yield. ¹H-NMR (400 MHz) (CD_3CN) δ (ppm): 8.21 (d, 2H, J = 4.76 Hz, pyrimidine); 6.91 (s, 1H, aromatic); 6.73 (s, 2H, aromatic); 6.50 (t, 1H, J = 4.80 Hz, pyrimidine); 5.72 (bs, 1H, pyrimidine-NH-); 3.80 (s, 3H, Ar-OCH₃); 3.63 (s, 2H, Ar-CH₂-NH-); 3.31 (q, 2H, J = 6.88 Hz, pyrimidine-NH-CH₂-); 2.53 (t, 2H, J = 6.96 Hz, Ar-CH₂-NH-CH₂-); 1.58-1.51 (m, 2H, -NH-CH₂-CH₂-); 1.49-1.42

(m, 2H, -NH-CH₂-CH₂-); 1.39-1.32 (m, 4H, -NH-CH₂-CH₂-CH₂-CH₂-CH₂-CH₂-NH-). ¹³C-NMR (100 MHz) (MeOD) δ (ppm): 163.5; 159.2; 149.2; 147.9; 128.2; 123.1; 116.3; 113.7; 111.0; 56.4; 53.4; 49.0; 42.0; 30.3; 28.8; 27.8; 27.7. ESI-MS (*m/z*): [M+H]⁺ = 330.60. I.R. (cm⁻¹): ν_{N-H}: 3261; finger print: 1284, 1258, 1158, 1130, 1034. m.p. = 87-89 °C. Anal. (C₁₈H₂₆N₄O₂) C, H, N Calcd: C 65.43 %, H 7.93 %, N 16.96 %; Found: C 65.41 %, H 7.92 %, N 17.00 %.

3-(((6-(pyrimidin-2-ylamino)hexyl)amino)methyl)phenol (19)

Compound **19** was prepared using *N*¹-(pyrimidin-2-yl)hexane-1,6-diamine (**4**) (0.117 g, 0.60 mmol), 3-hydroxybenzaldehyde (0.073 g, 0.60 mmol), NaBH₄ (0.068 g, 1.80 mmol), following the procedure 3 of GP-D described above. In this case the extraction was carried out with AcOEt instead of CH₂Cl₂. Column chromatography: silica gel, initially CH₂Cl₂/MeOH 1:1 (until the separation of the spot with R_f = 0.9) and subsequently CH₂Cl₂/MeOH/TEA 5:5:0.1, R_f = 0.67. After the chromatography the compound was purified by crystallization in CH₃CN. Pinkish solid, 0.104 g, 57% yield. ¹H-NMR (400 MHz) (Acetone-*d*₆) δ (ppm): 8.22 (d, 2H, *J* = 4.64 Hz, pyrimidine); 7.09 (t, 1H, *J* = 7.76 Hz, aromatic); 6.85 (s, 1H, aromatic); 6.79 (d, 1H, *J* = 7.52 Hz, aromatic); 6.67 (dd, 1H, *J*₁ = 8.00 Hz, *J*₂ = 1.80 Hz, aromatic); 6.50 (t, 1H, *J* = 4.76 Hz, pyrimidine); 6.22 (bs, 1H, pyrimidine-NH-); 3.67 (s, 2H, Ar-CH₂-NH-); 3.40-3.36 (m, 2H, pyrimidine-NH-CH₂-); 2.56 (t, 2H, 6.88 Hz, Ar-CH₂-NH-CH₂-); 1.64-1.57 (m, 2H, -NH-CH₂-CH₂-); 1.53-1.45 (m, 2H, -NH-CH₂-CH₂-); 1.43-1.37 (m, 4H, -NH-CH₂-CH₂-CH₂-CH₂-CH₂-NH-). ¹³C-NMR (100 MHz) (MeOD) δ (ppm): 163.5; 159.2; 158.8; 141.8; 130.5; 120.5; 116.4; 115.2; 111.0; 54.3; 49.7; 42.1; 30.4; 30.2; 28.1; 27.8. ESI-MS (*m/z*): [M+H]⁺ = 301.02. I.R. (cm⁻¹): ν_{N-H}: 3289; finger print: 1287, 1239, 1228, 1160, 927. m.p. = 75-77 °C. Anal. (C₁₇H₂₄N₄O) C, H, N Calcd: C 67.97 %, H 8.05 %, N 18.65 %; Found: C 68.03 %, H 8.04 %, N 18.61 %.

3-(((6-(pyrimidin-2-ylamino)hexyl)amino)methyl)benzene-1,2-diol (20)

Compound **20** was prepared using *N*¹-(pyrimidin-2-yl)hexane-1,6-diamine (**4**) (0.152 g, 0.78 mmol), 2,3-dihydroxybenzaldehyde (0.108 g, 0.78 mmol), NaBH₄ (0.089 g, 2.34 mmol), following the procedure 3 of GP-D described above. The compound was purified by crystallization in CH₃CN. Pinkish solid, 0.145 g, 59% yield. ¹H-NMR (400 MHz) (*d*₆-DMSO) δ (ppm): 8.22 (d, 2H, *J* = 4.72 Hz, pyrimidine); 7.08 (t, 1H, *J* = 5.60 Hz, pyrimidine-NH-); 6.61 (dd, 1H, *J*₁ = 7.48 Hz, *J*₂ = 1.88 Hz, aromatic); 6.52-6.46 (m, 3H, 2H aromatic and 1H pyrimidine); 3.80 (s, 2H, Ar-CH₂-NH-); 3.24 (q, 2H, *J* = 6.52 Hz, pyrimidine-NH-CH₂-); 1.53-1.41 (m, 4H, -NH-CH₂-CH₂-CH₂-CH₂-CH₂-CH₂-NH-); 1.31-1.29 (m, 4H, -NH-CH₂-CH₂-CH₂-CH₂-CH₂-NH-). * Ar-CH₂-NH-CH₂- covered by *d*₆-DMSO. ¹³C-NMR (100 MHz) (MeOD) δ (ppm): 163.5; 159.2; 147.7; 146.9; 123.6; 121.1; 119.4; 115.6; 111.0; 51.4; 48.9; 42.0; 30.3; 29.5; 27.8; 27.6. ESI-MS (*m/z*): [M+H]⁺ = 316.87. I.R. (cm⁻¹): finger print: 1289, 1194, 1102, 1068, 936. m.p. = 99-101 °C. Anal. (C₁₇H₂₄N₄O₂) C, H, N Calcd: C 64.53 %, H 7.65 %, N 17.71 %; Found: C 64.56 %, H 7.68 %, N 17.67 %.

***N*¹-((2,6-dichloropyridin-4-yl)methyl)-*N*⁶-(pyrimidin-2-yl)hexane-1,6-diamine (**21**)**

Compound **21** was prepared using *N*¹-(pyrimidin-2-yl)hexane-1,6-diamine (**4**) (0.117 g, 0.60 mmol), 2,6-dichloropyridine-4-carbaldehyde (0.106 g, 0.60 mmol), K₂CO₃ (1.659 g, 12.0 mmol), NaBH₄ (0.068 g, 1.8 mmol), following the procedure 1 of GP-D described above. Column chromatography: silica gel, AcOEt/MeOH 9:1, R_f = 0.4. White solid, 0.119 g, 57% yield. ¹H-NMR (400 MHz) (CD₃CN) δ (ppm): 8.21 (d, 2H, *J* = 4.76 Hz, pyrimidine); 7.36 (s, 2H, pyridine); 6.50 (t, 1H, *J* = 4.76 Hz, pyrimidine); 5.69 (bs, 1H, pyrimidine-NH-); 3.74 (s, 2H, pyridine-CH₂-NH-); 3.32 (q, 2H, *J* = 6.84 Hz, pyrimidine-NH-CH₂-); 2.51 (t, 2H, *J* = 6.88 Hz, pyridine-CH₂-NH-CH₂-); 1.59-1.52 (m, 2H, -NH-CH₂-CH₂-); 1.49-1.42 (m, 2H, -NH-CH₂-CH₂-); 1.39-1.33 (m, 4H, -NH-CH₂-CH₂-CH₂-CH₂-CH₂-NH-). ¹³C-NMR (100 MHz) (MeOD) δ (ppm): 163.5; 159.2; 157.8; 151.5; 123.6; 111.0; 52.4; 50.1; 42.1; 30.5; 30.4; 28.1; 27.9. ESI-MS (*m/z*): [M+H]⁺ = 353.98 (100); 355.91 (65); 356.97 (10). I.R. (cm⁻¹): ν_{N-H}: 3235;

finger print: 1216, 1155, 1129, 987. m.p. = 68-70 °C. Anal. (C₁₆H₂₁Cl₂N₅) C, H, N Calcd: C 54.24 %, H 5.97 %, N 19.77 %; Found: C 54.17 %, H 5.95 %, N 19.82 %.

***N*¹-((1*H*-indol-3-yl)methyl)-*N*⁶-(pyrimidin-2-yl)hexane-1,6-diamine (22)**

Compound **22** was prepared using *N*¹-(pyrimidin-2-yl)hexane-1,6-diamine (**4**) (0.076 g, 0.39 mmol), 1*H*-indole-3-carbaldehyde (0.057 g, 0.39 mmol), NaBH₄ (0.044 g, 1.17 mmol), following the procedure 2 of GP-D described above. Column chromatography: silica gel, initially MeOH (until the separation of the spot with R_f = 0.77) and subsequently MeOH/TEA 10:0.2, R_f = 0.20. After the chromatography the compound was filtered with CH₂Cl₂ to remove silica. Orange oil, 0.044 g, 36% yield. ¹H-NMR (400 MHz) (CD₃CN) δ (ppm): 9.18 (bs, 1H, indole-NH-); 8.21 (d, 2H, *J* = 4.76 Hz, pyrimidine); 7.62 (d, 1H, *J* = 7.92 Hz, indole); 7.38 (d, 1H, *J* = 8.12 Hz, indole); 7.15-7.10 (m, 2H, indole); 7.05-7.00 (m, 1H, indole); 6.50 (t, 1H, *J* = 4.76 Hz, pyrimidine); 5.70 (bs, 1H, pyrimidine-NH-); 3.89 (s, 2H, indole-CH₂-NH-); 3.30 (q, 2H, *J* = 6.88 Hz, pyrimidine-NH-CH₂-); 2.60 (t, 2H, *J* = 7.00 Hz, indole-CH₂-NH-CH₂-); 1.58-1.44 (m, 4H, -NH-CH₂-CH₂-CH₂-CH₂-CH₂-NH-); 1.39-1.32 (m, 4H, -NH-CH₂-CH₂-CH₂-CH₂-CH₂-NH-). ¹³C-NMR (100 MHz) (CDCl₃) δ (ppm): 162.5; 158.1; 136.4; 127.2; 123.4; 122.2; 119.7; 118.7; 113.5; 111.4; 110.4; 49.0; 44.3; 41.5; 29.5; 29.4; 27.1; 26.8. ESI-MS (*m/z*): [M+H]⁺ = 323.67. I.R. (cm⁻¹): ν_{N-H}: 3259; finger print: 1236, 1100, 1074, 1010, 983. Anal. (C₁₉H₂₅N₅) C, H, N Calcd: C 70.56 %, H 7.79 %, N 21.65 %; Found: C 70.47 %, H 7.81 %, N 21.72 %.

***N*¹-benzyl-*N*⁵-(pyridin-2-yl)pentane-1,5-diamine (23)**

Compound **23** was prepared using *N*¹-(pyridin-2-yl)pentane-1,5-diamine (**7**) (0.086 g, 0.48 mmol), benzaldehyde (49 μL, d=1.045 g/mL, 0.48 mmol), K₂CO₃ (1.327 g, 9.6 mmol), NaBH₄ (0.054 g, 1.44 mmol), following the procedure 1 of GP-D described above. Column chromatography: silica gel, CH₂Cl₂/MeOH 1:1, R_f = 0.36. Yellow oil, 0.071 g, 55% yield. ¹H-NMR (400 MHz) (CD₃CN) δ (ppm): 7.96 (dd, 1H, *J*₁ = 4.96 Hz, *J*₂ = 1.04 Hz, pyridine); 7.39-

7.34 (m, 1H, pyridine); 7.33-7.20 (m, 5H, aromatic); 6.48 (ddd, 1H, $J_1 = 6.96$ Hz, $J_2 = 5.04$ Hz, $J_3 = 0.76$ Hz, pyridine); 6.40 (d, 1H, $J = 8.44$ Hz, pyridine); 5.09 (s, 1H, pyridine-NH-); 3.72 (s, 2H, Ar-CH₂-NH-); 3.23 (q, 2H, $J = 6.92$ Hz, pyridine-NH-CH₂-); 2.55 (t, 2H, $J = 6.92$ Hz, Ar-CH₂-NH-CH₂-); 1.59-1.46 (m, 4H, -NH-CH₂-CH₂-CH₂-CH₂-NH-); 1.43-1.35 (m, 2H, -NH-CH₂-CH₂-CH₂-CH₂-NH-). ¹³C-NMR (100 MHz) (MeOD) δ (ppm): 160.4; 147.8; 140.4; 138.7; 129.6; 129.5; 128.2; 112.9; 109.7; 54.4; 49.8; 42.5; 30.3; 30.0; 25.8. ESI-MS (m/z): $[M+H]^+ = 270.00$. I.R. (cm⁻¹): ν_{N-H} : 3286; finger print: 1289, 1152, 982. Anal. (C₁₇H₂₃N₃) C, H, N Calcd: C 75.80 %, H 8.61 %, N 15.60 %; Found: C 75.86 %, H 8.59 %, N 15.55 %.

***N*¹-(4-bromobenzyl)-*N*⁵-(pyridin-2-yl)pentane-1,5-diamine (24)**

Compound **24** was prepared using *N*¹-(pyridin-2-yl)pentane-1,5-diamine (**7**) (0.075 g, 0.42 mmol), 4-bromobenzaldehyde (0.078 g, 0.42 mmol), K₂CO₃ (1.161 g, 8.4 mmol), NaBH₄ (0.048 g, 1.26 mmol), following the procedure 1 of GP-D described above. Column chromatography: silica gel, AcOEt/MeOH 1:1, $R_f = 0.33$. White solid, 0.070 g, 48% yield. ¹H-NMR (400 MHz) (CD₃CN) δ (ppm): 7.96 (dd, 1H, $J_1 = 4.92$ Hz, $J_2 = 1.04$ Hz, pyridine); 7.45 (d, 2H, $J = 8.32$ Hz, aromatic); 7.39-7.34 (m, 1H, pyridine); 7.25 (d, 2H, $J = 8.36$ Hz, aromatic); 6.50-6.47 (m, 1H, pyridine); 6.40 (d, 1H, $J = 8.40$ Hz, pyridine); 5.07 (bs, 1H, pyridine-NH-); 3.68 (s, 2H, Ar-CH₂-NH-); 3.23 (q, 2H, $J = 6.88$ Hz, pyridine-NH-CH₂-); 2.53 (t, 2H, $J = 6.84$ Hz, Ar-CH₂-NH-CH₂-); 1.59-1.35 (m, 6H, -NH-CH₂-CH₂-CH₂-CH₂-CH₂-NH-). ¹³C-NMR (100 MHz) (MeOD) δ (ppm): 160.4; 147.8; 140.0; 138.7; 132.5; 131.5; 121.8; 112.9; 109.7; 53.7; 49.8; 42.5; 30.3; 30.2; 25.8. ESI-MS (m/z): $[M+H]^+ = 347.54$ (100); 349.60 (90). I.R. (cm⁻¹): ν_{N-H} : 3284; finger print: 1287, 1156, 1135, 1069, 1009, 980. m.p. = 65-68 °C. Anal. (C₁₇H₂₂BrN₃) C, H, N Calcd: C 58.63 %, H 6.37 %, N 12.07 %; Found: C 58.59 %, H 6.36 %, N 12.04 %.

***N*¹-benzyl-*N*⁶-(pyridin-2-yl)hexane-1,6-diamine (25)**

Compound **25** was prepared using *N*¹-(pyridin-2-yl)hexane-1,6-diamine (**8**) (0.106 g, 0.55 mmol), benzaldehyde (56 μ L, $d=1.045$ g/mL, 0.55 mmol), K₂CO₃ (1.520 g, 11.0 mmol), NaBH₄ (0.062 g, 1.65 mmol), following the procedure 1 of GP-D described above. Column chromatography: silica gel, CH₂Cl₂/MeOH 7:3, R_f = 0.3. Yellow oil, 0.083 g, 53% yield. ¹H-NMR (400 MHz) (CD₃CN) δ (ppm): 7.96 (dd, 1H, $J_1 = 5.00$ Hz, $J_2 = 1.08$ Hz, pyridine); 7.39-7.34 (m, 1H, pyridine); 7.33-7.20 (m, 5H, aromatic); 6.48 (ddd, 1H, $J_1 = 7.00$ Hz, $J_2 = 5.08$ Hz, $J_3 = 0.80$ Hz, pyridine); 6.40 (d, 1H, $J = 8.44$ Hz, pyridine); 5.10 (bs, 1H, pyridine-NH-); 3.72 (s, 2H, Ar-CH₂-NH-); 3.23 (q, 2H, $J = 6.88$ Hz, pyridine-NH-CH₂-); 2.54 (t, 2H, $J = 6.96$ Hz, Ar-CH₂-NH-CH₂-); 1.59-1.52 (m, 2H, -NH-CH₂-CH₂-); 1.50-1.43 (m, 2H, -NH-CH₂-CH₂-); 1.40-1.27 (m, 4H, -NH-CH₂-CH₂-CH₂-CH₂-CH₂-NH-). ¹³C-NMR (100 MHz) (CD₃CN) δ (ppm): 160.2; 148.8; 142.2; 137.8; 129.1; 129.0; 127.5; 112.8; 108.1; 54.3; 49.9; 42.2; 30.7; 30.2; 27.8; 27.6. ESI-MS (m/z): [M+H]⁺ = 283.98. I.R. (cm⁻¹): $\nu_{\text{N-H}}$: 3279; finger print: 1288, 1152, 982. Anal. (C₁₈H₂₅N₃) C, H, N Calcd: C 76.28 %, H 8.89 %, N 14.83 %; Found: C 76.33 %, H 8.87 %, N 14.80 %.

***N*¹-(4-bromobenzyl)-*N*⁶-(pyridin-2-yl)hexane-1,6-diamine (**26**)**

Compound **26** was prepared using *N*¹-(pyridin-2-yl)hexane-1,6-diamine (**8**) (0.110 g, 0.57 mmol), 4-bromobenzaldehyde (0.106 g, 0.57 mmol), K₂CO₃ (1.576 g, 11.4 mmol), NaBH₄ (0.065 g, 1.71 mmol), following the procedure 1 of GP-D described above. Column chromatography: silica gel, CH₂Cl₂/MeOH 1:1, R_f = 0.38. Yellow solid, 0.084 g, 40% yield. ¹H-NMR (400 MHz) (CD₃CN) δ (ppm): 7.96 (dd, 1H, $J_1 = 4.96$ Hz, $J_2 = 1.08$ Hz, pyridine); 7.47 (d, 2H, $J = 8.36$ Hz, aromatic); 7.39-7.34 (m, 1H, pyridine); 7.25 (d, 2H, $J = 8.44$ Hz, aromatic); 6.48 (ddd, 1H, $J_1 = 7.00$ Hz, $J_2 = 5.04$ Hz, $J_3 = 0.80$ Hz, pyridine); 6.40 (d, 1H, $J = 8.44$ Hz, pyridine); 5.08 (bs, 1H, pyridine-NH-); 3.68 (s, 2H, Ar-CH₂-NH-); 3.22 (q, 2H, $J = 6.92$ Hz, pyridine-NH-CH₂-); 2.51 (t, 2H, $J = 6.88$ Hz, Ar-CH₂-NH-CH₂-); 1.59-1.51 (m, 2H, -NH-CH₂-CH₂-); 1.49-1.42 (m, 2H, -NH-CH₂-CH₂-); 1.40-1.27 (m, 4H, -NH-CH₂-CH₂-CH₂-

CH₂-CH₂-CH₂-NH-). ¹³C-NMR (100 MHz) (CD₃CN) δ (ppm): 160.2; 148.8; 141.8; 137.8; 132.0; 131.0; 120.6; 112.8; 108.1; 53.5; 49.8; 42.2; 30.7; 30.2; 27.8; 27.6. ESI-MS (*m/z*): [M+H]⁺ = 361.76 (90), 363.95 (100). I.R. (cm⁻¹): ν_{N-H}: 3269; finger print: 1156, 1109, 1067, 1011, 979. m.p. = 42-44 °C. Anal. (C₁₈H₂₄BrN₃) C, H, N Calcd: C 59.67 %, H 6.68 %, N 11.60 %; Found: C 59.69 %, H 6.69 %, N 11.63 %.

***N*¹-(4-chlorobenzyl)-*N*⁶-(pyridin-2-yl)hexane-1,6-diamine (27)**

Compound **27** was prepared using *N*¹-(pyridin-2-yl)hexane-1,6-diamine (**8**) (0.108 g, 0.56 mmol), 4-chlorobenzaldehyde (0.079 g, 0.56 mmol), K₂CO₃ (1.548 g, 11.2 mmol), NaBH₄ (0.064 g, 1.68 mmol), following the procedure 1 of GP-D described above. Column chromatography: silica gel, CH₂Cl₂/MeOH 1:1, R_f = 0.31. Yellow solid, 0.090 g, 51% yield. ¹H-NMR (400 MHz) (CD₃CN) δ (ppm): 7.96 (d, 1H, *J* = 4.96 Hz, pyridine); 7.36 (t, 1H, *J* = 8.00 Hz, pyridine); 7.31 (s, 4H, aromatic); 6.48 (t, 1H, *J* = 6.00 Hz, pyridine); 6.40 (d, 1H, *J* = 8.44 Hz, pyridine); 5.07 (bs, 1H, pyridine-NH-); 3.70 (s, 2H, Ar-CH₂-NH-); 3.23 (q, 2H, *J* = 6.56 Hz, pyridine-NH-CH₂-); 2.52 (t, 2H, *J* = 6.80 Hz, Ar-CH₂-NH-CH₂-); 1.59-1.52 (m, 2H, -NH-CH₂-CH₂-); 1.49-1.42 (m, 2H, -NH-CH₂-CH₂-); 1.40-1.27 (m, 4H, -NH-CH₂-CH₂-CH₂-CH₂-CH₂-NH-). ¹³C-NMR (100 MHz) (CD₃CN) δ (ppm): 160.2; 148.8; 141.3; 137.8; 132.6; 130.6; 129.0; 112.8; 108.1; 53.5; 49.8; 42.2; 30.7; 30.1; 27.8; 27.6. ESI-MS (*m/z*): [M+H]⁺ = 318.13 (100); 320.13 (35). I.R. (cm⁻¹): ν_{N-H}: 3261; finger print: 1296, 1156, 1121, 1091, 1084, 1015, 982. m.p. = 41-43 °C. Anal. (C₁₈H₂₄ClN₃) C, H, N Calcd: C 68.02 %, H 7.61 %, N 13.22 %; Found: C 67.97 %, H 7.59 %, N 13.26 %.

***N*¹-(2-methoxybenzyl)-*N*⁶-(pyridin-2-yl)hexane-1,6-diamine (28)**

Compound **28** was prepared using *N*¹-(pyridin-2-yl)hexane-1,6-diamine (**8**) (0.106 g, 0.55 mmol), 2-methoxybenzaldehyde (0.075 g, 0.55 mmol), K₂CO₃ (1.520 g, 11.0 mmol), NaBH₄ (0.062 g, 1.65 mmol), following the procedure 1 of GP-D described above. Column chromatography: silica gel, CH₂Cl₂/MeOH 7:3, R_f = 0.2. Yellow oil, 0.112 g, 65% yield. ¹H-

NMR (400 MHz) (CD₃CN) δ (ppm): 7.96 (dd, 1H, $J_1 = 4.96$ Hz, $J_2 = 1.08$ Hz, pyridine); 7.38-7.34 (m, 1H, pyridine); 7.26-7.20 (m, 2H, aromatic); 6.94-6.88 (m, 2H, aromatic); 6.48 (ddd, 1H, $J_1 = 6.96$ Hz, $J_2 = 5.04$ Hz, $J_3 = 0.80$ Hz, pyridine); 6.40 (d, 1H, $J = 8.44$ Hz, pyridine); 5.07 (bs, 1H, pyridine-NH-); 3.80 (s, 3H, Ar-OCH₃); 3.68 (s, 2H, Ar-CH₂-NH-); 3.23 (q, 2H, $J = 6.92$ Hz, pyridine-NH-CH₂-); 2.52 (t, 2H, $J = 6.92$ Hz, Ar-CH₂-NH-CH₂-); 1.59-1.52 (m, 2H, -NH-CH₂-CH₂-); 1.49-1.42 (m, 2H, -NH-CH₂-CH₂-); 1.40-1.27 (m, 4H, -NH-CH₂-CH₂-CH₂-CH₂-CH₂-NH-). ¹³C-NMR (100 MHz) (CD₃CN) δ (ppm): 160.2; 158.5; 148.8; 137.8; 130.2; 129.9; 128.8; 121.1; 112.8; 111.3; 108.1; 55.9; 49.9; 49.3; 42.2; 30.7; 30.2; 27.8; 27.7. ESI-MS (m/z): [M+H]⁺ = 313.88. I.R. (cm⁻¹): $\nu_{\text{N-H}}$: 3281; finger print: 1289, 1239, 1151, 1100, 1050, 1029, 982. Anal. (C₁₉H₂₇N₃O) C, H, N Calcd: C 72.81 %, H 8.68 %, N 13.41 %; Found: C 72.82 %, H 8.71 %, N 13.38 %.

***N*¹-(pyridin-2-yl)-*N*⁶-(3,4,5-trimethoxybenzyl)hexane-1,6-diamine (29)**

Compound **29** was prepared using *N*¹-(pyridin-2-yl)hexane-1,6-diamine (**8**) (0.102 g, 0.53 mmol), 3,4,5-trimethoxybenzaldehyde (0.104 g, 0.53 mmol), NaBH₄ (0.060 g, 1.59 mmol), following the procedure 3 of GP-D described above. Column chromatography: silica gel, AcOEt/MeOH/TEA 5:5:0.2, $R_f = 0.53$. Orange oil, 0.133 g, 67% yield. ¹H-NMR (400 MHz) (CD₃CN) δ (ppm): 7.97-7.96 (m, 1H, pyridine); 7.38-7.34 (m, 1H, pyridine); 6.62 (s, 2H, aromatic); 6.48 (ddd, 1H, $J_1 = 7.00$ Hz, $J_2 = 5.04$ Hz, $J_3 = 0.84$ Hz, pyridine); 6.40 (d, 1H, $J = 8.44$ Hz, pyridine); 5.07 (bs, 1H, pyridine-NH-); 3.79 (s, 6H, Ar-(OCH₃)₂); 3.68 (s, 3H, -OCH₃); 3.66 (s, 2H, Ar-CH₂-NH-); 3.23 (q, 2H, $J = 6.88$ Hz, pyridine-NH-CH₂-); 2.55 (t, 2H, $J = 6.88$ Hz, Ar-CH₂-NH-CH₂-); 1.59-1.52 (m, 2H, -NH-CH₂-CH₂-); 1.51-1.45 (m, 2H, -NH-CH₂-CH₂-); 1.41-1.27 (m, 4H, -NH-CH₂-CH₂-CH₂-CH₂-CH₂-NH-). ¹³C-NMR (100 MHz) (MeOD) δ (ppm): 160.5; 154.6; 147.8; 138.7; 138.5; 134.9; 112.9; 109.7; 107.1; 61.1; 56.6; 54.2; 49.5; 42.5; 30.3; 29.6; 28.0; 27.9. ESI-MS (m/z): [M+H]⁺ = 373.90. I.R. (cm⁻¹): $\nu_{\text{N-H}}$

H: 3295; finger print: 1234, 1121, 1006. Anal. (C₂₁H₃₁N₃O₃) C, H, N Calcd: C 67.53 %, H 8.37 %, N 11.25 %; Found: C 67.57 %, H 8.34 %, N 11.23 %.

2-methoxy-4-(((6-(pyridin-2-ylamino)hexyl)amino)methyl)phenol (30)

Compound **30** was prepared using *N*¹-(pyridin-2-yl)hexane-1,6-diamine (**8**) (0.102 g, 0.53 mmol), 4-hydroxy-3-methoxybenzaldehyde (0.081 g, 0.53 mmol), NaBH₄ (0.060 g, 1.59 mmol), following the procedure 3 of GP-D with some modifications: after the reaction with NaBH₄, the addition of HCl and the removal of the solvent, the residue was washed with warm AcOEt and then the solid was diluted with 20 mL of saturated aqueous solution of NaHCO₃ and extracted with AcOEt (3 x 20 mL). The organic layer was dried over Na₂SO₄ and the solvent was removed under vacuum. Yellow oil, 0.140 g, 80% yield. ¹H-NMR (400 MHz) (CD₃CN) δ (ppm): 7.96 (dd, 1H, *J*₁ = 5.04 Hz, *J*₂ = 1.12 Hz, pyridine); 7.39-7.34 (m, 1H, pyridine); 6.92 (s, 1H, aromatic); 6.74 (s, 2H, aromatic); 6.48 (ddd, 1H, *J*₁ = 7.00 Hz, *J*₂ = 5.04 Hz, *J*₃ = 0.80 Hz, pyridine); 6.40 (d, 1H, *J* = 8.40 Hz, pyridine); 5.08 (bs, 1H, pyridine-NH-); 3.82 (s, 3H, -OCH₃); 3.63 (s, 2H, Ar-CH₂-NH-); 3.23 (q, 2H, *J* = 6.92 Hz, pyridine-NH-CH₂-); 2.53 (t, 2H, *J* = 6.96 Hz, Ar-CH₂-NH-CH₂-); 1.59-1.52 (m, 2H, -NH-CH₂-CH₂-); 1.50-1.43 (m, 2H, -NH-CH₂-CH₂-); 1.40-1.27 (m, 4H, -NH-CH₂-CH₂-CH₂-CH₂-CH₂-CH₂-NH-). ¹³C-NMR (100 MHz) (MeOD) δ (ppm): 160.5; 149.1; 147.8; 147.3; 138.7; 130.4; 122.7; 116.2; 113.4; 112.9; 109.7; 56.4; 54.0; 49.4; 42.5; 30.3; 29.7; 28.1; 27.9. ESI-MS (*m/z*): [M+H]⁺ = 330.20. I.R. (cm⁻¹): finger print: 1274, 1152, 1125, 1033, 982. Anal. (C₁₉H₂₇N₃O₂) C, H, N Calcd: C 69.27 %, H 8.26 %, N 12.76 %; Found: C 69.19 %, H 8.28 %, N 12.80 %.

3-(((6-(pyridin-2-ylamino)hexyl)amino)methyl)phenol (31)

Compound **31** was prepared using *N*¹-(pyridin-2-yl)hexane-1,6-diamine (**8**) (0.075 g, 0.39 mmol), 3-hydroxybenzaldehyde (0.048 g, 0.39 mmol), NaBH₄ (0.044 g, 1.17 mmol), following the procedure 3 of GP-D described above. In this case the extraction was carried out with AcOEt instead of CH₂Cl₂. Column chromatography: silica gel, AcOEt/MeOH/TEA 5:5:0.1, R_f

= 0.22. White solid, 0.062 g, 53% yield. ¹H-NMR (400 MHz) (Acetone-*d*₆) δ (ppm): 7.98-7.96 (m, 1H, pyridine); 7.36-7.32 (m, 1H, pyridine); 7.09 (t, 1H, *J* = 7.80 Hz, aromatic); 6.86 (s, 1H, aromatic); 6.79 (d, 1H, *J* = 7.52, aromatic); 6.67 (dd, 1H, *J*₁ = 7.84 Hz, *J*₂ = 1.80 Hz, aromatic); 6.46-6.43 (m, 2H, pyridine); 5.64 (bs, 1H, pyridine-NH-); 3.67 (s, 2H, Ar-CH₂-NH-); 3.33-3.28 (m, 2H, pyridine-NH-CH₂-); 2.56 (t, 2H, *J* = 6.88 Hz, Ar-CH₂-NH-CH₂-); 1.63-1.56 (m, 2H, -NH-CH₂-CH₂-); 1.53-1.46 (m, 2H, -NH-CH₂-CH₂-); 1.43-1.34 (m, 4H, -NH-CH₂-CH₂-CH₂-CH₂-NH-). ¹³C-NMR (100 MHz) (MeOD) δ (ppm): 160.4; 158.9; 147.8; 140.4; 138.7; 130.6; 120.7; 116.6; 115.6; 112.9; 109.7; 53.9; 49.5; 42.5; 30.3; 29.6; 28.0; 27.9. ESI-MS (*m/z*): [M+H]⁺ = 300.40. I.R. (cm⁻¹): ν_{N-H}: 3270; finger print: 1281, 1153, 1112, 926. m.p. = 86-88°C. Anal. (C₁₈H₂₅N₃O) C, H, N Calcd: C 72.21 %, H 8.42 %, N 14.03 %; Found: C 72.17 %, H 8.44 %, N 14.06 %.

3-(((6-(pyridin-2-ylamino)hexyl)amino)methyl)benzene-1,2-diol (**32**)

Compound **32** was prepared using *N*¹-(pyridin-2-yl)hexane-1,6-diamine (**8**) (0.102 g, 0.53 mmol), 2,3-dihydroxybenzaldehyde (0.073 g, 0.53 mmol), NaBH₄ (0.060 g, 1.59 mmol), following the procedure 1 of GP-D described above. The compound was purified by washing with CH₃CN. White solid, 0.084 g, 50% yield. ¹H-NMR (400 MHz) (MeOD) δ (ppm): 7.89-7.88 (m, 1H, pyridine); 7.42-7.38 (m, 1H, pyridine); 6.69 (t, 1H, *J* = 4.64 Hz, aromatic); 6.56 (d, 2H, *J* = 4.68 Hz, aromatic); 6.52-6.48 (m, 2H, pyridine); 3.90 (s, 2H, Ar-CH₂-NH-); 3.24 (t, 2H, *J* = 7.04 Hz, pyridine-NH-CH₂-); 2.67 (t, 2H, *J* = 7.16 Hz, Ar-CH₂-NH-CH₂-); 1.64-1.55 (m, 4H, -NH-CH₂-CH₂-CH₂-CH₂-CH₂-CH₂-); 1.42-1.40 (m, 4H, -NH-CH₂-CH₂-CH₂-CH₂-CH₂-CH₂-NH-). ¹³C-NMR (100 MHz) (*d*₆-DMSO) δ (ppm): 159.0; 147.6; 146.0; 145.2; 136.5; 123.7; 118.8; 118.0; 114.3; 111.2; 107.9; 51.1; 48.0; 40.7; 29.0; 28.9; 26.59; 26.55. ESI-MS (*m/z*): [M+H]⁺ = 315.92. I.R. (cm⁻¹): finger print: 1292, 1280, 1199, 1067. m.p. = 112-114 °C. Anal. (C₁₈H₂₅N₃O₂) C, H, N Calcd: C 68.54 %, H 7.99 %, N 13.32 %; Found: C 68.61 %, H 7.98 %, N 13.28 %.

***N*¹-((2,6-dichloropyridin-4-yl)methyl)-*N*⁶-(pyridin-2-yl)hexane-1,6-diamine (33)**

Compound **33** was prepared using *N*¹-(pyridin-2-yl)hexane-1,6-diamine (**8**) (0.108 g, 0.56 mmol), 2,6-dichloropyridine-4-carbaldehyde (0.099 g, 0.56 mmol), K₂CO₃ (1.548 g, 11.2 mmol), NaBH₄ (0.064 g, 1.68 mmol), following the procedure 1 of GP-D described above. Column chromatography: silica gel, AcOEt/MeOH 9.5:0.5, R_f = 0.32. White solid, 0.131 g, 66% yield. ¹H-NMR (400 MHz) (CD₃CN) δ (ppm): 7.96 (dd, 1H, *J*₁ = 4.96 Hz, *J*₂ = 1.04 Hz, pyridine); 7.39-7.24 (m, 3H, 1H pyridine and 2H 2,6-dichloropyridine); 6.48 (ddd, 1H, *J*₁ = 6.96 Hz, *J*₂ = 5.04 Hz, *J*₃ = 0.80 Hz, pyridine); 6.40 (d, 1H, *J* = 8.40 Hz, pyridine); 5.07 (bs, 1H, pyridine-NH-); 3.75 (s, 2H, 2,6-dichloropyridine-CH₂-NH-); 3.23 (q, 2H, *J* = 6.92 Hz, pyridine-NH-CH₂-); 2.51 (t, 2H, *J* = 6.84 Hz, 2,6-dichloropyridine-CH₂-NH-CH₂-); 1.59-1.52 (m, 2H, -NH-CH₂-CH₂-); 1.49-1.43 (m, 2H, -NH-CH₂-CH₂-); 1.41-1.27 (m, 4H, -NH-CH₂-CH₂-CH₂-CH₂-CH₂-NH-). ¹³C-NMR (100 MHz) (MeOD) δ (ppm): 160.5; 157.8; 151.5; 147.8; 138.7; 123.6; 112.9; 109.7; 52.4; 50.1; 42.6; 30.5; 30.4; 28.1; 28.0. ESI-MS (*m/z*): [M+H]⁺ = 353.05 (90), 354.98 (100), 356.91 (15). I.R. (cm⁻¹): ν_{N-H}: 3237; finger print: 1246, 1212, 1154, 1128, 1085, 986. m.p. = 61-64 °C. Anal. (C₁₇H₂₂Cl₂N₄) C, H, N Calcd: C 57.79 %, H 6.28 %, N 15.86 %; Found: C 57.83 %, H 6.30 %, N 15.81 %.

Enzymatic assays

Materials and methods

Electric eel AChE (*EeAChE*, EC 3.1.1.7), *equine* BChE (EC 3.1.1.8), acetylthiocholine iodide, 5,5'-dithio-bis-(2-nitrobenzoic acid) (DTNB), tacrine and donepezil, used as reference standard, were purchased from Sigma-Aldrich (Milan, Italy). All other chemical and biological reagents and solvents used were of the highest analytical, commercially available grade. The water, utilized for the preparation of the phosphate buffer and of the compounds solutions, was distilled and filtered on nylon membrane filters with 0.2 μm pore size with the Millipore®

Filtration apparatus before each use. Micropipettes Labmate (BRAND Dig. 10-100 μL ; Dig. 100-1000 μL ; Dig. 0.1-2 μL) and Transferpette (HIGH TECH LAB LM200: 20-200 μL ; LM5000: 1000-5000 μL) were used to collect the samples. The assays were carried out by double beam UV-Vis Lambda 40 Perkin Elmer spectrophotometer, using optical polystyrene cuvettes (10x10x45 mm, 340–800 nm optical transparency), each measure was repeated at least in triplicate. For data processing UV-WIN Lab version 2.0, Perkin Elmer Corporation and SigmaPlot version 8.02 were used. The spectrophotometric method of Ellman²⁵ with minor modifications was used to evaluate the inhibition of ChEs. This method is based on the reaction of released thiocholine to give a coloured product, at wavelength of 412 nm, with the chromogenic reagent DTNB. The absorbance was recorded at 412 nm between 0 and 1.6 minutes and the absorbance variation, utilized for the kinetic assay, was measured between 0.5 and 1.5 minutes to allow stabilization of the UV-Vis lamp and of the solution. The method is extremely sensitive to variations in the order of microliters: the standard deviations (less than 5%) of the values obtained are compatible with the experimental errors associated with the use of micropipettes. Each compound tested was dissolved in the opportune quantity of DMSO in order to obtain a final cuvette DMSO content < 0.033%, that does not affect the enzyme activity. *EeAChE* and *eqBChE* were periodically tested to evaluate the effective enzymatic activity.

Percent inhibition of EeAChE and eqBChE

For all the synthesized compounds the percentages of inhibition towards AChE of *Electrophorus electricus* (*EeAChE*) and equine BChE (*eqBChE*) were evaluated.

3.0 mL of a solution in 0.1 M phosphate buffer (pH = 7.4) containing DTNB (0.25 mM) and *EeAChE* (0.083 U mL^{-1}) or *eqBChE* (0.083 U mL^{-1}) were placed in a polystyrene cuvette of 1.0 cm path length; 1 μL of a solution in DMSO of the tested compound was added to obtain in cuvette concentration range 9 μM – 0.09 μM . With this solution the blank was made. To start

the reaction 30 μL of a solution in 0.1 M phosphate buffer (pH = 7.4) of acetylthiocholine (10 mM) were added in order to obtain a final concentration of acetylthiocholine equal to 100 μM . The increase in the absorbance, due to the production of the yellow 2-nitro-5-thiobenzoic anion, was recorded at 412 nm at 25 $^{\circ}\text{C}$, and the absorbance variation was measured between 0.5 and 1.5 min. As a control, an identical solution of the enzyme without the inhibitor was processed following the same protocol to determine the 100% of enzyme activity. Each experiment was repeated at least in triplicate. The potency of each compound to inhibit *EeAChE* or *eqBChE* activity was expressed as percent inhibition calculated using the following equation:

$$\text{Inhibition (\%)} = \frac{A_c - A_i}{A_c} \times 100$$

where A_i and A_c represent the average of absorbance variation in presence of inhibitor and without inhibitor, respectively.

Determination of constant and mechanism of inhibition vs EeAChE and eqBChE

The constants and the mechanisms of inhibition were determined for a selection of compounds, among the most potent as inhibitors of *EeAChE* and *eqBChE* (**9**, **13**, **19**, **23**, **25** and **28** towards *EeAChE*; **18**, **22**, **25**, **26**, **28** and **30** towards *eqBChE*). For each compound a stock solution 500 μM was prepared in $\text{H}_2\text{O}/\text{DMSO}$ or in 10^{-2} M HCl and diluted in water to prepare solutions of opportune concentrations such as to introduce in the cuvette volumes ranging from 30 to 100 μL , to obtain the desired final concentrations. The maximum amount of DMSO used for the preparation of the stock solution was calculated in order to have a DMSO content in cuvette <0.033%.

3.0 mL of 0.1 M phosphate buffer (pH = 7.4) containing DTNB (0.25 mM) and *EeAChE* (0.083 U mL^{-1}) or *eqBChE* (0.083 U mL^{-1}) were mixed with the opportune volume of inhibitor solution, in order to obtain a final inhibitor concentration in cuvette between 90 and 1800 nM. With this solution the blank was made. The reaction was started by adding to the enzyme–inhibitor mixture the proper volume of a solution in 0.1 M phosphate buffer (pH = 7.4) of

acetylthiocholine (10 mM), in order to obtain a final concentration of substrate equal to 100-400 μM . Each determination was repeated for five times. The absorbance variations were measured at 412 nm at 25 °C between 0.5 and 1.5 min. From these data the values of the enzymatic hydrolysis rate, expressed as μmol of substrate hydrolyzed in one minute by an enzymatic unit, were obtained.

In order to determine the inhibition constants (K_i) and the inhibition mechanisms the rates of hydrolysis at three different concentrations of substrate in presence of five different concentrations of inhibitor were measured. The recorded data were analyzed by the enzyme kinetic module of SigmaPlot (version 8.02) plotting the reciprocal of rate of hydrolysis ($1/v$, $\text{min}/\mu\text{M}$) vs the concentration of inhibitor (nM), according to the Dixon's method²⁶ in order to find the best fitting model of inhibition, as indicated by calculated linear regression coefficient R^2 .

Determination of IC_{50} vs $EeAChE$ for compound **20**, tacrine and donepezil

The IC_{50} value of compound **20** vs $EeAChE$ and the IC_{50} values of tacrine and donepezil vs both ChEs were calculated. For this purpose, eight different inhibitor solutions were prepared. For compound **20**, solutions in 10^{-2} M HCl were prepared, having suitable concentrations, so as to add 20 μL of these solutions to the assay mixture, to obtain a final concentration between 0.05 and 10 μM ; for tacrine and donepezil, solutions in DMSO were prepared, having suitable concentrations, so as to add 1 μL of these solutions to the assay mixture, to obtain a final concentration between 0.5 and 27000 nM. For each inhibitor concentration the percentage of inhibition in presence of $EeAChE$ or $eqBChE$ (0.0833 U mL^{-1}) and acetylthiocholine (100 μM) was measured as described above. The recorded data were analyzed by the enzyme kinetic module of SigmaPlot plotting the percentages of inhibition as a function of the different concentrations of inhibitor, expressed in logarithmic scale, in order to obtain the sigmoid graph,

from which it was possible to determinate the IC₅₀ value of the tested compound. The IC₅₀ was confirmed by repeating the experiment twice.

Computational studies and ADME prediction

All computational studies were carried out by means of Schrödinger Suite 2018-1.⁴⁰ The x-ray crystallographic structures of the *hAChE* in complex to donepezil (PDB code: 4EY7)¹³ and the *hBChE* in complex to the naphamide derivative (PDB code: 5NN0)²⁷ were used. *hChEs* structures were prepared by using Maestro Protein Preparation Wizard⁴¹ tool and were refined to optimize hydrogen-bonds and energy minimized by using OPLS_2005 as force field at pH 7.4.⁴²⁻⁴⁴ The homology between the human and not human ChEs isoforms used for the enzymatic assays was assessed by the sequence alignment performed by Prime.⁴⁵

All derivatives were submitted to 5000 steps of Monte Carlo conformational search applied to all rotatable bonds. The water solvent effect was considered using the implicit model GB/SA.⁴⁶ The global minimum energy structures were used to carry out molecular docking simulations.

Then, target binding sites were defined by means of a regular grid box of about 27,000 Å³ centred on the catalytic serine residues. All docking simulations were computed using Glide⁴⁷ ligand flexible algorithm at standard-precision (SP) level. The best docked poses of the most potent inhibitors resulted by *in vitro* assays of pyrimidine and pyridine derivatives were submitted to 250 ns of molecular dynamics (MDs) simulations by using Desmond ver. 4.2.⁴⁸ The system was solvated in SPC explicit solvent model and counter ions were added to neutralize the system net charge. After optimization of the solvated model, we relaxed the system with Martyna-Tobias_Klein isobaric-isothermal ensemble (MTK_NPT). This preliminary stage included two energy minimizations of 2000 steps: in the first run, the system was restrained with a force constant of 50 kcal mol⁻¹ Å⁻¹, while in the second one all the system was released without any restrains. The following conditions for MDs were used: NPT

ensemble, a temperature of 300 K, a pressure of 1 bar, with the Berendsen thermostat-barostat, a recording interval equal to 250 ps both for energy and for trajectory collecting 1000 frames for each simulation.

In order to identify possible PAINS, all synthesized final molecules were screened using *in silico* public tools available at <https://zinc15.docking.org/patterns/home/> and <http://www.swissadme.ch/>.

ADME descriptors of the most potent compounds were predicted using SwissADME public server.³⁶ The following ADME parameters have been selected: Molecular Weight (MW); number H-bond acceptors (H-b acc); number H-bond donors (H-b don); number of heavy atoms (heavy atoms); number rotatable bonds (rot bonds); Topological Polar Surface Area in Å² (TPSA); Octanol/Water partition coefficient (MLogP); water solubility (LogS ESOL); water solubility class (Sol class); gastrointestinal absorption (GI); blood-brain barrier permeation (BBB); number of Lipinski's rule of five violations (Lipinski viol).³⁷

Chelation studies

Materials and methods

FeCl₃·6H₂O, CuSO₄·5H₂O, Zn(NO₃)₂·6H₂O and MeOH, used for chelation studies, were purchased from Sigma-Aldrich. Micropipettes Labmate (BRAND Dig. 10-100 µL; Dig. 100-1000 µL) and Transferpette (HIGH TECH LAB LM200: 20-200 µL; LM5000: 1000-5000 µL) were used to collect the samples. The assays were carried out by double beam UV-Vis Lambda 40 Perkin Elmer spectrophotometer, using quartz cuvettes (Optech, type S/Q/10). Data were elaborated using UV-WIN Lab Version 2.0, Perkin Elmer Corporation, Microsoft Excel 2010 and Spekwin32.

UV-Vis titration

For the UV-Vis titration ligand solutions in MeOH were prepared: 10^{-3} M for compounds **9**, **13**, **20**, **25**, **28**, **30**; $5 \cdot 10^{-3}$ M for compounds **18** and **19**. Stock solutions 1 M of $\text{CuSO}_4 \cdot 5\text{H}_2\text{O}$ and $\text{Zn}(\text{NO}_3)_2 \cdot 6\text{H}_2\text{O}$ in water and 0.1 M of $\text{FeCl}_3 \cdot 6\text{H}_2\text{O}$ in MeOH were prepared and diluted with MeOH to obtain different solutions, having suitable concentrations, so as to add 2.85 mL of these solutions to 150 μL of ligand solution, to obtain in 3 mL of assay mixture a final molar ratio of metal ion to ligand between 0.1 and 20. UV-Vis spectra were recorded from 210 to 450 nm.

For the first measure 150 μL of ligand solution were diluted in 2.85 mL of MeOH into sample cuvette, while only MeOH was placed in reference cuvette and the UV-Vis spectrum was recorded. For the subsequent measurements 2.85 mL of the opportune metal solution were placed both in sample cuvette and in reference cuvette; then 150 μL of ligand solution were added to sample cuvette, while 150 μL of MeOH were added to reference cuvette and the UV-Vis spectra were recorded. The spectra thus obtained were superimposed to observe the variations present between the ligand alone and in presence of increasing amount of metal.

Job's Plot

To determine the stoichiometric coefficients of the complexes the Job's method³³ was used, which requires to mix, in appropriate proportions, equimolar solution of metal ion and ligand, so that the final volume and the total moles present in the cuvette are equal for each measurement. The absorbance values were recorded at the wavelengths, extrapolated from the UV-Vis titration spectra, where the maximum variation of absorbance was observed. At the same time two solutions in MeOH of equal concentration were prepared, one of ligand and one of metal ion, diluting the solutions 1 M of $\text{CuSO}_4 \cdot 5\text{H}_2\text{O}$ and $\text{Zn}(\text{NO}_3)_2 \cdot 6\text{H}_2\text{O}$ and 0.1 M of $\text{FeCl}_3 \cdot 6\text{H}_2\text{O}$ previously prepared. The concentrations of the solutions used and the wavelengths in which the absorbance was recorded were: $4.96 \cdot 10^{-4}$ M for **18** and Fe^{3+} – 258, 375 nm; $5.02 \cdot 10^{-4}$ M for **18** and Cu^{2+} – 330 nm; $5.66 \cdot 10^{-4}$ M for **19** and Fe^{3+} – 292, 375 nm; $5.66 \cdot 10^{-4}$

M for **19** and Cu^{2+} – 312, 330 nm; $3.10 \cdot 10^{-4}$ M for **20** and Fe^{3+} – 370 nm; $3.35 \cdot 10^{-4}$ M for **20** and Cu^{2+} – 330 nm; $3.00 \cdot 10^{-4}$ M for **25** and Fe^{3+} – 251, 318 nm; $3.99 \cdot 10^{-4}$ M for **25** and Cu^{2+} – 330 nm; $3.00 \cdot 10^{-4}$ M for **28** and Fe^{3+} – 316, 374 nm; $3.99 \cdot 10^{-4}$ M for **28** and Cu^{2+} – 330 nm; $3.28 \cdot 10^{-4}$ M for **30** and Fe^{3+} – 310, 372 nm; $3.58 \cdot 10^{-4}$ M for **30** and Cu^{2+} – 312, 330 nm.

For each determination 9-24 measurements were made, introducing appropriate volumes of metal and ligand solutions in the sample cuvette to obtain mole fractions of the ligand in the range 0.1-0.95, while appropriate volumes of ligand solution and MeOH were placed in the reference cuvette, to obtain the same concentration of ligand in the sample cuvette. The absorbance values of the metal ion, calculated by the Lambert-Beer relation, known the extinction coefficients ϵ of the metal ion at used wavelengths and the nominal concentrations of the metal ion for each measure, were algebraically subtracted from the recorded absorbance values, in order to obtain the exclusive absorbance variations due to the complex formation. The resulting ΔA were reported in graph as a function of the mole fraction of the ligand and through the intersections of the linear regression lines, the mole fraction X, which caused the maximum variation in absorbance, was determined and used to calculate the value of the coefficient n, which corresponds to the number of ligand molecules per cation, applying the following equation:

$$n = \frac{X}{1 - X}$$

Antioxidant activity

Materials and methods

2,2-Diphenyl-1-picrylhydrazyl (DPPH), MeOH, ascorbic acid, used as reference standard, were purchased from Sigma-Aldrich. Micropipettes Labmate (BRAND Dig. 10-100 μL ; Dig. 100-1000 μL) and Transferpette (HIGH TECH LAB LM200: 20-200 μL ; LM5000: 1000-5000 μL) were used to collect the samples. The assays were carried out by double beam UV-Vis

Lambda 40 Perkin Elmer spectrophotometer, using optical polystyrene cuvettes (10x10x45 mm, 340–800 nm optical transparency); each measure was repeated at least in triplicate. For data processing UV-WIN Lab version 2.0, Perkin Elmer Corporation was used. The antioxidant activity of the tested compounds was evaluated by the DPPH method,³⁴ based on the ability of antioxidant compounds to react with the stable radical DPPH, which has a maximum absorption at about 515 nm. Thus, by measuring the decrease in absorbance over time of DPPH solutions to which increasing amounts of the tested compound are added, the antioxidant activity of the compound can be determined.

Antioxidant activity tests

To assess the antioxidant activity of **18**, **19**, **20** and **30**, at first the decrease in absorbance over time at 515 nm of a solution of DPPH and tested compound was recorded, until the completion of the reaction. To 2.90 mL of MeOH, 60 μ L of a DPPH solution in MeOH (~1.2 mM) and 40 μ L of an antioxidant solution in MeOH (4.5 mM) were added, in order to have in cuvette concentrations of DPPH equal to about 25 μ M and of antioxidant equal to 60 μ M. The exact DPPH concentration was calculated through the Lambert-Beer relation, known the extinction coefficient of DPPH at 515 nm, equal to $1.25 \cdot 10^4$.³⁴ The absorbance was recorded until the plateau was reached.

Subsequently, for compounds that showed antioxidant activity (**18**, **20** and **30**) the EC₅₀ values were determined. To obtain the initial DPPH concentration, 2.94 mL of MeOH and 60 μ L of DPPH solution in MeOH (~1.2 mM) were placed in a polystyrene cuvette and the absorbance was recorded at 515 nm. The exact initial DPPH concentration was calculated through the Lambert-Beer relation. For subsequent measurements the cuvettes were set up by introducing the opportune volume of MeOH to reach a total volume of 3 mL, 60 μ L of DPPH solution in MeOH (~1.2 mM, to have a final concentration of ~25 μ M) and the appropriate volumes of antioxidant stock solution in MeOH, to have final concentrations between 1.5 μ M

and 12 μM for **20** and between 5 μM and 60 μM for **18** and **30**; the absorbance was recorded at 515 nm at the plateau, then after 1 minute for compound **20**, after 90 minutes for compounds **18** and **30**. Each measure was repeated four times. With absorbance data the percentages of residual DPPH at steady state were obtained, using the following equation:

$$\% \text{ residual DPPH} = \frac{Ac}{A0} \times 100$$

where Ac is the average of absorbance in presence of antioxidant at plateau and $A0$ is the average of initial absorbance of DPPH.

Plotting the percentage of residual DPPH at the steady state as a function of molar ratio of antioxidant to initial DPPH, it is possible to obtain the value of EC_{50} , defined as the ratio of moles of antioxidant which reduce by 50% the initial concentration of DPPH to initial moles of DPPH. The whole experiment was repeated twice for each compound. The same procedure was performed using ascorbic acid as antioxidant, at cuvette concentrations between 1.5 μM and 18 μM , recording the absorbance at 515 nm after 2 minutes from the preparation of the cuvettes. In this way an EC_{50} equal to 0.265 ± 0.007 was measured, in accordance with literature.⁴⁹

Inhibition of amyloid and Tau aggregation

Cloning and over-expression of A β_{42} peptide

E. coli competent cells BL21 (DE3) were transformed with the pET28a vector (Novagen, Inc., Madison, WI, USA) carrying the DNA sequence of A β_{42} . Because of the addition of the initiation codon ATG in front of both genes, the overexpressed peptide contains an additional methionine residue at its N terminus. For overnight culture preparation, an amount of 10 mL of M9 minimal medium containing 50 $\mu\text{g}\cdot\text{mL}^{-1}$ of kanamycin was inoculated with a colony of BL21 (DE3) bearing the plasmid to be expressed at 37 °C. For expression of the A β_{42} peptide,

the required volume of overnight culture to obtain 1:500 dilution was added into fresh M9 minimal medium containing $50 \mu\text{g}\cdot\text{mL}^{-1}$ of kanamycin and $250 \mu\text{M}$ Th-S. The bacterial culture was grown at 37°C and 250 rpm. When the cell density reached $\text{OD}_{600} = 0.6$, an amount of 980 μL of culture was transferred into Eppendorf tubes of 1.5 mL with 10 μL of each compound to be tested in DMSO and 10 μL of isopropyl 1-thio- β -D-galactopyranoside (IPTG) at 100 mM. The final concentration of drug was fixed at 100 μM . The samples were grown overnight at 37°C and 1400 rpm using a Thermomixer (Eppendorf, Hamburg, Germany). As negative control (maximal amyloid presence) the same amount of DMSO without drug was added in the sample. In parallel, non-induced samples (in absence of IPTG) were also prepared and used as positive controls (non-amyloid presence). In addition, these samples were used to assess the potential intrinsic toxicity of the compounds and to confirm the correct bacterial growth.

Cloning and Overexpression of Tau Protein

E. coli BL21 (DE3) competent cells were transformed with pTARA containing the RNA-polymerase gen of T7 phage (T7RP) under the control of the promoter PBAD. *E. coli* BL21 (DE3) with pTARA competent cells were transformed with pRKT42 vector encoding four repeats of tau protein in two inserts. For overnight culture preparation, 10 mL of M9 medium containing 0.5% of glucose, $50 \mu\text{g}\cdot\text{mL}^{-1}$ of ampicillin, and $12.5 \mu\text{g}\cdot\text{mL}^{-1}$ of chloramphenicol were inoculated with a colony of BL21 (DE3) bearing the plasmids to be expressed at 37°C . For expression of tau protein, the required volume of overnight culture to obtain 1:500 dilution was added to fresh M9 minimal medium containing 0.5% of glucose, $50 \mu\text{g}\cdot\text{mL}^{-1}$ of ampicillin, $12.5 \mu\text{g}\cdot\text{mL}^{-1}$ of chloramphenicol, and $250 \mu\text{M}$ Th-S. The bacterial culture was grown at 37°C and 250 rpm. When the cell density reached $\text{OD}_{600} = 0.6$, an amount of 980 μL of culture was transferred into Eppendorf tubes of 1.5 mL with 10 μL of each compound to be tested in DMSO and 10 μL of arabinose at 25%. The final concentration of drug was fixed at 100 μM . The samples were grown overnight at 37°C and 1400 rpm using a Thermomixer (Eppendorf,

Hamburg, Germany). As negative control (maximal presence of tau), the same amount of DMSO without drug was added in the sample. In parallel, non-induced samples (in absence of arabinose) were also prepared and used as positive controls (absence of tau). In addition, these samples were used to assess the potential intrinsic toxicity of the compounds and to confirm the correct bacterial growth.

Thioflavin S (Th-S) Steady-State Fluorescence

Th-S (T1892) and other chemical reagents were purchased from Sigma (St. Louis, MO). Th-S stock solution (2500 mM) was prepared in double-distilled water purified through a Milli-Q system (Millipore, USA). ThS fluorescence and absorbance were tracked using a DTX 800 plate reader Multimode Detector equipped with a Multimode Analysis Software (Beckman-Coulter, USA). Filters of 430/35 and 485/20 nm were used for the excitation and emission wavelengths, respectively. 535/25 nm filters were also used for the absorbance determination. In order to normalize the Th-S fluorescence as a function of the bacterial concentration, OD600 was obtained using a Shimadzu UV-2401 PC UV-Vis spectrophotometer (Shimadzu, Japan). Note that the fluorescence normalization was carried out considering as 100% the Th-S fluorescence of the bacterial cells expressing the peptide or protein in the absence of drug and 0% the Th-S fluorescence of the bacterial cells non-expressing the peptide or protein. A minimum of 5 independent assays (with three replicates for assay) were performed for each tested compound. More assays were performed to obtain a SEM < 5% with a maximum of 10 independent assays.

Cytotoxicity assays

The compounds **9**, **13**, **19**, **20**, **22**, **23**, **25**, **26** and **28** were evaluated for cell viability effects using the MTT assay. Briefly, U-87 MG Cell Line from human brain (glioblastoma astrocytoma) (ATCC, Manassas, VA, USA) were seeded into 96-well microtiter plates (NunclonTM, Nunc, Germany) at a density of $1.5 \cdot 10^4$ cells/well.^{50, 51} After 24 h cells were

exposed to increased concentrations of tested compounds (1, 5, 10 and 50 μM) in cell culture medium. After an incubation time of 24 h, medium was replaced by new fresh containing 0.5 mg/mL MTT (Sigma, Deisenhofen, Germany). After 2 h at 37 $^{\circ}\text{C}$ in 5% CO_2 unreacted dye was removed and cells were dissolved by DMSO (Merck, Darmstadt, Germany). Absorbance was read at 570 nm by a microtiter spectrophotometer plate reader. The data were expressed as absorbance relative to untreated cells in the same experiment and standardized to 100%. All data points were performed in triplicate and at least three independent experiments.

ASSOCIATED CONTENT

Supporting Information. The Supporting Information is available free of charge on the ACS Publications website at DOI:

Figures S1-S46, Table S1 (DOCX)

Molecular formula strings and some data (CSV)

AUTHOR INFORMATION

Corresponding Authors

***Luigi Scipione** – *Department of Scienze di Base e Applicate per l'Ingegneria, Sapienza University of Rome, via Castro Laurenziano 7, I-00161, Rome, Italy; phone: +39-06-49913737; Email: luigi.scipione@uniroma1.it.*

***Stefano Alcaro** – *Net4Science s.r.l., Campus universitario "S. Venuta", Viale Europa, 88100, Catanzaro, Italy; Dipartimento di Scienze della Salute, Università "Magna Græcia" di Catanzaro, Viale Europa, 88100, Catanzaro, Italy; phone: +39-0961-3694198; Email: alcaro@unicz.it.*

Authors

Martina Bortolami – *Department of Scienze di Base e Applicate per l’Ingegneria, Sapienza University of Rome, via Castro Laurenziano 7, I-00161, Rome, Italy*

Fabiana Pandolfi – *Department of Scienze di Base e Applicate per l’Ingegneria, Sapienza University of Rome, via Castro Laurenziano 7, I-00161, Rome, Italy*

Valeria Tudino – *Department of Chimica e Tecnologia del Farmaco, Sapienza University of Rome, Piazzale Aldo Moro 5, 00185, Rome, Italy*

Antonella Messori – *Department of Chimica e Tecnologia del Farmaco, Sapienza University of Rome, Piazzale Aldo Moro 5, 00185, Rome, Italy*

Valentina Noemi Madia – *Department of Chimica e Tecnologia del Farmaco, Sapienza University of Rome, Piazzale Aldo Moro 5, 00185, Rome, Italy*

Daniela De Vita – *Department of Environmental Biology, Sapienza University of Rome, Piazzale Aldo Moro 5, 00185, Rome, Italy*

Roberto Di Santo – *Department of Scienze di Base e Applicate per l’Ingegneria, Sapienza University of Rome, via Castro Laurenziano 7, I-00161, Rome, Italy; Istituto Pasteur, Fondazione Cenci Bolognetti, Department of Chemistry and Technology of Drug, Sapienza University of Rome, Piazzale Aldo Moro 5, 00185, Rome, Italy*

Roberta Costi – *Department of Scienze di Base e Applicate per l’Ingegneria, Sapienza University of Rome, via Castro Laurenziano 7, I-00161, Rome, Italy; Istituto Pasteur, Fondazione Cenci Bolognetti, Department of Chemistry and Technology of Drug, Sapienza University of Rome, Piazzale Aldo Moro 5, 00185, Rome, Italy*

Isabella Romeo – *Net4Science s.r.l., Campus universitario “S. Venuta”, Viale Europa, 88100, Catanzaro, Italy; Dipartimento di Scienze della Salute, Università “Magna Græcia” di Catanzaro, Viale Europa, 88100, Catanzaro, Italy*

Marisa Colone – *National Center for Drug Research and Evaluation, Istituto Superiore di Sanità, Viale Regina Elena, 00161, Rome, Italy*

Annarita Stringaro – *National Center for Drug Research and Evaluation, Istituto Superiore di Sanità, Viale Regina Elena, 00161, Rome, Italy*

Alba Espargaró – *Department of Pharmacy and Pharmaceutical Technology and Physical-Chemistry, Faculty of Pharmacy and Food Sciences, University of Barcelona, Avda. Joan XXIII, 27-31 Barcelona, Catalonia, Spain*

Raimon Sabatè *Department of Pharmacy and Pharmaceutical Technology and Physical-Chemistry, Faculty of Pharmacy and Food Sciences, University of Barcelona, Avda. Joan XXIII, 27-31 Barcelona, Catalonia, Spain*

Author Contributions

The manuscript was written through contributions of all authors. All authors have given approval to the final version of the manuscript.

Notes

The authors declare that they have no known competing financial interests or personal relationships that could have appeared to influence the work reported in this paper.

ACKNOWLEDGMENT

This work was financially supported by the Italian Ministry for Education, Universities and Research (MIUR), Sapienza University of Rome and by Istituto Superiore di Sanità, ISS (Ministry of Health - ISS funding).

ABBREVIATIONS USED

AD, Alzheimer's disease; ACh, acetylcholine; A β , β -amyloid peptide; ChAT, choline acetyl transferase; ChEIs, cholinesterase inhibitors; ChEs, cholinesterases; FDA, Food and Drug Administration; AChE, acetylcholinesterase; BChE, butyrylcholinesterase; CAS, catalytic active site; PAS, peripheral anionic site; *hAChE*, human AChE; *hBChE*, human BChE; TEA, triethylamine; TFA, trifluoroacetic acid; DMF, dimethylformamide; *EeAChE*, *Electrophorus electricus* AChE; *eqBChE*, equine BChE; K_i, inhibition constant; RMSD, Root Mean Square Deviation; MD, molecular dynamics; DPPH, 2,2-diphenyl-1-picrylhydrazyl; TPSA, Topological Polar Surface Area in Å²; MLogP, octanol/water partition coefficient; LogS ESOL, water solubility; GI, gastrointestinal absorption; BBB, Blood-Brain Barrier permeation; PAINS, Pan Assay INterference compounds.

REFERENCES

1. Alzheimer's News Today. Alzheimer's Disease Statistics. <https://alzheimersnewstoday.com/alzheimers-disease-statistics> (accessed May 17, 2021).
2. Wimo, A.; Guerchet, M.; Ali, G. C.; Wu, Y. T.; Prina, A. M.; Winblad, B.; Jönsson, L.; Liu, Z.; Prince, M. The worldwide costs of dementia 2015 and comparisons with 2010. *Alzheimers Dement.* **2017**, *13*, 1-7.
3. Prince, M. J.; Wimo, A.; Guerchet, M. M.; Ali, G. C.; Wu, Y.-T.; Prina, M. *The Global Impact of Dementia: an Analysis of Prevalence, Incidence, Cost and Trends*; World Alzheimer Report 2015; Alzheimer's Disease International: London, UK, September 2015.
4. Du, X.; Wang, X.; Geng, M. Alzheimer's disease hypothesis and related therapies. *Transl. Neurodegener.* **2018**, *7*, 1-7.
5. Coyle, J. T.; Price, D. L.; Delong, M. R. Alzheimer's disease: a disorder of cortical cholinergic innervation. *Science* **1983**, *219*, 1184-1190.

6. Whitehouse, P. J.; Price, D. L.; Clark, A. W.; Coyle, J. T.; DeLong, M. R. Alzheimer disease: evidence for selective loss of cholinergic neurons in the nucleus basalis. *Ann. Neurol.* **1981**, *10*, 122-126.
7. Bowen, D. M.; Smith, C. B.; White, P.; Davison, A. N. Neurotransmitter-related enzymes and indices of hypoxia in senile dementia and other abiotrophies. *Brain* **1976**, *99*, 459-496.
8. Drachman, D. A.; Leavitt, J. Human memory and the cholinergic system: a relationship to aging? *Arch. Neurol.* **1974**, *30*, 113-121.
9. Marucci, G.; Buccioni, M.; Dal Ben, D.; Lambertucci, C.; Volpini, R.; Amenta, F. Efficacy of acetylcholinesterase inhibitors in Alzheimer's disease. *Neuropharmacology* **2020**, *190*, 108352.
10. Greig, N. H.; Utsuki, T.; Yu, Q.-s.; Zhu, X.; Holloway, H. W.; Perry, T.; Lee, B.; Ingram, D. K.; Lahiri, D. K. A new therapeutic target in Alzheimer's disease treatment: attention to butyrylcholinesterase. *Curr. Med. Res. Opin.* **2001**, *17*, 159-165.
11. Mesulam, M.-M.; Guillozet, A.; Shaw, P.; Levey, A.; Duysen, E.; Lockridge, O. Acetylcholinesterase knockouts establish central cholinergic pathways and can use butyrylcholinesterase to hydrolyze acetylcholine. *Neuroscience* **2002**, *110*, 627-639.
12. Brus, B.; Kosak, U.; Turk, S.; Pisljar, A.; Coquelle, N.; Kos, J.; Stojan, J.; Colletier, J.-P.; Gobec, S. Discovery, biological evaluation, and crystal structure of a novel nanomolar selective butyrylcholinesterase inhibitor. *J. Med. Chem.* **2014**, *57*, 8167-8179.
13. Cheung, J.; Rudolph, M. J.; Burshteyn, F.; Cassidy, M. S.; Gary, E. N.; Love, J.; Franklin, M. C.; Height, J. J. Structures of human acetylcholinesterase in complex with pharmacologically important ligands. *J. Med. Chem.* **2012**, *55*, 10282-10286.
14. Rosenberry, T. L.; Brazzolotto, X.; Macdonald, I. R.; Wandhammer, M.; Trovaslet-Leroy, M.; Darvesh, S.; Nachon, F. Comparison of the binding of reversible inhibitors to human

- butyrylcholinesterase and acetylcholinesterase: A crystallographic, kinetic and calorimetric study. *Molecules* **2017**, *22*, 2098.
15. Silman, I.; Sussman, J. L. Acetylcholinesterase: 'classical' and 'non-classical' functions and pharmacology. *Curr. Opin. Pharmacol.* **2005**, *5*, 293-302.
 16. Bartolini, M.; Bertucci, C.; Cavrini, V.; Andrisano, V. β -Amyloid aggregation induced by human acetylcholinesterase: inhibition studies. *Biochem. Pharmacol.* **2003**, *65*, 407-416.
 17. Rees, T.; Hammond, P.; Soreq, H.; Younkin, S.; Brimijoin, S. Acetylcholinesterase promotes beta-amyloid plaques in cerebral cortex. *Neurobiol. Aging* **2003**, *24*, 777-787.
 18. Wang, H.; Zhang, H. Reconsideration of anticholinesterase therapeutic strategies against Alzheimer's disease. *ACS Chem. Neurosci.* **2018**, *10*, 852-862.
 19. Zhang, P.; Xu, S.; Zhu, Z.; Xu, J. Multi-target design strategies for the improved treatment of Alzheimer's disease. *Eur. J. Med. Chem.* **2019**, *176*, 228-247.
 20. Bortolami, M.; Rocco, D.; Messori, A.; Di Santo, R.; Costi, R.; Madia, V. N.; Scipione, L.; Pandolfi, F. Acetylcholinesterase inhibitors for the treatment of Alzheimer's disease-a patent review (2016-present). *Expert Opin. Ther. Pat.* **2021**, *31*, 399-420.
 21. Maramai, S.; Benchekroun, M.; Gabr, M. T.; Yahiaoui, S. Multitarget therapeutic strategies for Alzheimer's disease: Review on emerging target combinations. *BioMed Res. Int.l* **2020**, *2020*, 5120230.
 22. Pandolfi, F.; De Vita, D.; Bortolami, M.; Coluccia, A.; Di Santo, R.; Costi, R.; Andrisano, V.; Alabiso, F.; Bergamini, C.; Fato, R. New pyridine derivatives as inhibitors of acetylcholinesterase and amyloid aggregation. *Eur. J. Med. Chem.* **2017**, *141*, 197-210.
 23. Bortolami, M.; Pandolfi, F.; De Vita, D.; Carafa, C.; Messori, A.; Di Santo, R.; Feroci, M.; Costi, R.; Chiarotto, I.; Bagetta, D. New deferiprone derivatives as multi-functional cholinesterase inhibitors: design, synthesis and in vitro evaluation. *Eur. J. Med. Chem.* **2020**, *198*, 112350.

24. Shafir, A.; Buchwald, S. L. Highly selective room-temperature copper-catalyzed C–N coupling reactions. *J. Am. Chem. Soc.* **2006**, *128*, 8742-8743.
25. Ellman, G. L.; Courtney, K. D.; Andres Jr, V.; Featherstone, R. M. A new and rapid colorimetric determination of acetylcholinesterase activity. *Biochem. Pharmacol.* **1961**, *7*, 88-95.
26. Dixon, M. The determination of enzyme inhibitor constants. *Biochem. J.* **1953**, *55*, 170-171.
27. Kosak, U.; Brus, B.; Knez, D.; Zakelj, S.; Trontelj, J.; Pisljar, A.; Sink, R.; Jukič, M.; Zivin, M.; Podkova, A. The magic of crystal structure-based inhibitor optimization: development of a butyrylcholinesterase inhibitor with picomolar affinity and in vivo activity. *J. Med. Chem.* **2018**, *61*, 119-139.
28. Warren, G. L.; Do, T. D.; Kelley, B. P.; Nicholls, A.; Warren, S. D. Essential considerations for using protein–ligand structures in drug discovery. *Drug Discov. Today* **2012**, *17*, 1270-1281.
29. Warren, G. L.; Andrews, C. W.; Capelli, A.-M.; Clarke, B.; LaLonde, J.; Lambert, M. H.; Lindvall, M.; Nevins, N.; Semus, S. F.; Senger, S. A critical assessment of docking programs and scoring functions. *J. Med. Chem.* **2006**, *49*, 5912-5931.
30. Saccoliti, F.; Madia, V. N.; Tudino, V.; De Leo, A.; Pescatori, L.; Messori, A.; De Vita, D.; Scipione, L.; Brun, R.; Kaiser, M. Design, synthesis, and biological evaluation of new 1-(aryl-1*H*-pyrrolyl)(phenyl)methyl-1*H*-imidazole derivatives as antiprotozoal agents. *J. Med. Chem.* **2019**, *62*, 1330-1347.
31. Balasubramanian, K. Quantum chemical insights into Alzheimer's disease: Curcumin's chelation with Cu (II), Zn (II), and Pd (II) as a mechanism for its prevention. *Int. J. Quantum Chem.* **2016**, *116*, 1107-1119.

32. Catapano, M. C.; Tvrđý, V.; Karličková, J.; Migkos, T.; Valentová, K.; Křen, V.; Mladěnka, P. The stoichiometry of isoquercitrin complex with iron or copper is highly dependent on experimental conditions. *Nutrients* **2017**, *9*, 1193.
33. Job, P. Formation and stability of inorganic complexes in solution. *Ann. Chim.* **1928**, *9*, 113-203.
34. Molyneux, P. The use of the stable free radical diphenylpicrylhydrazyl (DPPH) for estimating antioxidant activity. *Songklanakarín J. Sci. Technol.* **2004**, *26*, 211-219.
35. Espargaró, A.; Medina, A.; Di Pietro, O.; Muñoz-Torrero, D.; Sabate, R. Ultra rapid in vivo screening for anti-Alzheimer anti-amyloid drugs. *Sci. Rep.* **2016**, *6*, 1-8.
36. Daina, A.; Michielin, O.; Zoete, V. SwissADME: a free web tool to evaluate pharmacokinetics, drug-likeness and medicinal chemistry friendliness of small molecules. *Sci. Rep.* **2017**, *7*, 1-13.
37. Lipinski, C. A.; Lombardo, F.; Dominy, B. W.; Feeney, P. J. Experimental and computational approaches to estimate solubility and permeability in drug discovery and development settings. *Adv. Drug Deliv. Rev.* **1997**, *23*, 3-25.
38. Baell, J.; Walters, M. A. Chemistry: chemical con artists foil drug discovery. *Nature* **2014**, *513*, 481.
39. Kowalczyk, J.; Grapsi, E.; Espargaró, A.; Caballero, A. B.; Juárez-Jiménez, J.; Busquets, M. A.; Gamez, P.; Sabate, R.; Estelrich, J. Dual effect of prussian blue nanoparticles on A β 40 aggregation: β -Sheet fibril reduction and copper dyshomeostasis regulation. *Biomacromolecules* **2021**, *22*, 430-440.
40. Schrödinger Release 2018-1. *Schrödinger Suite*; Schrödinger, LLC: New York, 2018.
41. Schrödinger Release 2018-1. *Maestro*; Schrödinger, LLC: New York, 2018.

42. Jorgensen, W. L.; Maxwell, D. S.; Tirado-Rives, J. Development and testing of the OPLS all-atom force field on conformational energetics and properties of organic liquids. *J. Am. Chem. Soc.* **1996**, *118*, 11225-11236.
43. Sastry, G. M.; Adzhigirey, M.; Day, T.; Annabhimoju, R.; Sherman, W. Protein and ligand preparation: parameters, protocols, and influence on virtual screening enrichments. *J. Comput. Aided Mol. Des.* **2013**, *27*, 221-234.
44. Crucitti, G. C.; Pescatori, L.; Messori, A.; Madia, V. N.; Pupo, G.; Saccoliti, F.; Scipione, L.; Tortorella, S.; Di Leva, F. S.; Cosconati, S. Discovery of *N*-aryl-naphthylamines as *in vitro* inhibitors of the interaction between HIV integrase and the cofactor LEDGF/p75. *Eur. J. Med. Chem.* **2015**, *101*, 288-294.
45. Schrödinger Release 2018-1: *Prime*; Schrödinger, LLC: New York, 2018.
46. Hasel, W.; Hendrickson, T. F.; Still, W. C. A rapid approximation to the solvent accessible surface areas of atoms. *Tetrahedron Comput. Methodol.* **1988**, *1*, 103-116.
47. Schrödinger Release 2018-1: *Glide*; Schrödinger, LLC: New York, 2018.
48. *Desmond Molecular Dynamics System*, version 4.2; D. E. Shaw Research: New York, 2018.
49. Brand-Williams, W.; Cuvelier, M.-E.; Berset, C. Use of a free radical method to evaluate antioxidant activity. *LWT* **1995**, *28*, 25-30.
50. Taglieri, L.; Saccoliti, F.; Nicolai, A.; Peruzzi, G.; Madia, V. N.; Tudino, V.; Messori, A.; Di Santo, R.; Artico, M.; Taurone, S. Discovery of a pyrimidine compound endowed with antitumor activity. *Invest. New Drugs* **2020**, *38*, 39-49.
51. Madia, V. N.; Nicolai, A.; Messori, A.; De Leo, A.; Ialongo, D.; Tudino, V.; Saccoliti, F.; De Vita, D.; Scipione, L.; Artico, M. Design, synthesis and biological evaluation of new pyrimidine derivatives as anticancer agents. *Molecules* **2021**, *26*, 771.

Table of Contents Graphic

